Responses to the Comments of the Anonymous Referee #1

We appreciate the further useful comments and suggestions from this reviewer again. Our point-by-point responses to the reviewer's comments are as follows (the reviewer's comments are marked in Italic font). The tracking version of the manuscript is attached with this reply.

General comments:

The authors have put a lot of effort to improve the manuscript that is now clearer in terms of both presentation and analyses. However I recommend major changes to be made to consider the manuscript suitable for publication. Please refer to the detailed comments below to improve presentation of the results. Some restructuring of the manuscript is still needed especially in the methods/results sections.

Based on the reviewer's suggestion, the structure of the manuscript has been rearranged, especially in Section 2 and 4. Section 2.2 in the original manuscript has been removed and the contents have been merged into Section 2.1 and 4.1, respectively. In the revised version, Section 4.1 and 4.2 focus on the influence of different meteorological input datasets and different fire emission inventories on fire aerosol abundance separately.

Specific comments:

Line 62: A paper on health impacts from fires was recently published in Scientific Reports that could be worth citing (www.nature.com/articles/srep37074): "Population exposure to hazardous air quality due to the 2015 fires in Equatorial Asia" by P. Crippa, S. Castruccio, S. Archer-Nicholls, G. B. Lebron, M. Kuwata, A. Thota, S. Sumin, E. Butt, C. Wiedinmyer & D. V. Spracklen

Added.

Line 80: please rephrase "various climate variabilities...in different temporal scales"

The sentence has been modified to "Reid et al. (2012) investigated relationships between fire hotspot appearance and various weather phenomena as well as climate variabilities in different time scales over the MC, …"

Line 81: ENSO is actually "El Niño–Southern Oscillation" (remove "and" and type Niño correctly)

Corrected.

Line 133: replace "included" with "adopted"

Done.

Line 177-180: please rephrase the last part of the sentence

The sentence has been modified to "On the other hand, Sumatra (s2), Borneo (s3) and the rest of the Maritime Continent (s4) do not have clearly identifiable dry seasons and this contributes to the weaker correlation (Fig. 2b – d). Besides that, underground peatland burning may not be immediately extinguished by precipitation."

Line 181: The first part of this section still refers to model settings so should be merged with section 2.1. From Line 198 the authors are discussing model evaluation with respect to precipitation, so this discussion should be moved either at the beginning of the results or merged to section 4 when the influence of different meteorological boundary conditions is anlayzed. Please also consider summarizing it.

The first part of this section that discusses the design of numerical simulations has been merged to Section 2.1 "The model". The model evaluation with respect to precipitation has been moved to Section 4.1.

Line 324: "highlighted green areas" could be removed unless you explicitly refer to Figure 3.

Removed.

Line 408: change "in causing degradation of air quality" with "in degrading air quality"

Done.

Line 413: "haze event occurrence across from..." this part is not clear, please rephrase

The sentence has been changed to "Interestingly, the discrepancy of these two variables, however, has become smaller in recent years and even reversed in 2014, implying an increase of haze occurrence across cities with different populations in the region."

Line 419-422: You are not accounting for other anthropogenic emissions in your simulations, so this sentence should be supported by a literature reference and possibly linked to any evidence/results in your paper.

We added the IEA (2015) report to support our statement.

IEA: Energy and Climate Change, World Energy Outlook Special Report, International Energy Agency, pp. 74 -77, 2015.

Line 436: is this distance inferred from Figure 9? If so please refer to the figure or provide appropriate reference.

The sentence has been modified to "Fire aerosol plumes with concentrations higher than 0.1 μg m^{-3} can be transported westward as far as 7000 km from the burning sites (Fig. 9a)."

Line 482: wrong figure number. It should be Fig 7b and c.

Corrected.

Line 493: replace "similar to" with "similarly to", also in other parts of the manuscript

Corrected.

Line 494: It is not clear how you are able to infer the contribution from different regions. You should mention this somewhere in the methods. In general all the presented results should be supported by a clear explanation on how have been derived in an appropriate method section.

This was actually clearly described in the text in Section 2.1, as "In order to distinguish the spatial-temporal coverage and influence of biomass burning aerosols from different regions in Southeast Asia and nearby northern Australia, we have created five tracers to represent fire aerosols respectively from mainland Southeast Asia (s1), Sumatra and Java islands (s2), Borneo (s3), the rest of the Maritime Continent (s4), and northern Australia (s5) as illustrated in Fig. 1".

We now have added one more sentence to avoid any potential misunderstanding: "Based on this design, we are able to identify fire $PM_{2.5}$ concentration from different regions and estimate the contribution to the total fire $PM_{2.5}$ in a receptor city."

Line 496: Section 3.3 is too long and dispersive. The authors present the role of winds, wet scavenging, quantify the contribution of fire emissions to different regions/cities and finally introduce the role of different emission inventories. Please consider reorganizing and summarizing. The paragraph from line 496 could be moved to the model description or merged to the discussion on the emission inventories. You could separate these sections and have one for meteorological and one for emissions influence.

The paragraph from Line 496 has been moved to Section 4.2 with the discussion of the impact of different fire emission inventories on fire aerosol concentration.

Line 510: "wind field" should be "wind fields", check this through the paper.

Modified.

Line 514-523: this part could be integrated with the content in section 2.2 where the authors evaluate the model in terms of precipitation. However I recommend organizing a new section where the model evaluation is discussed.

We separated the discussion of meteorological datasets and fire emission inventories into Section 4.1 and 4.2.

Line 532: which "modelled results"? please be more specific/rephrase, also with respect to the subsequent sentence starting with "To examine such an influence".

The sentence has been modified to "In addition to meteorological inputs, using different fire emission estimates could also affect the modeled $PM_{2.5}$ concentration. To examine

this impact, we have compared two simulations with the same meteorological input but different fire emission inventories, the FNL_FINN using FINNv1.5 and FNL_GFED using GFEDv4.1s."

Line 548-549: please rephrase and be more specific on which modeled results you are referring to.

The sentence has been modified to "We would also like to point out the importance of spatiotemporal distribution of fire emission to the modeled $PM_{2.5}$ concentration."

Line 588: It would be better to summarize your findings instead of mentioning what you have done.

The sentence has been changed to "Based on these results, we suggest further research is needed to improve the current estimate of the spatiotemporal distribution of fire emissions, in addition to total emitted quantities from the fire hotspots"

From line 591: please check the use of tenses.

Checked.

Line 599: it would be good to add how many of these events were likely to be due to fires.

The sentence has been changed to "The top four cities in the HED ranking, Jakarta, Bangkok, Hanoi, and Yangon, with a total population exceeding two millions, all have experienced more than 200 days per year of low visibility due to particulate pollution over the past decade and more than 50% of those low visibility days were mainly due to fire aerosols."

Line 601: rephrase as "but also in those". "Pollutions" should be "pollution"

Done.

Line 602: please rephrase this sentence and link better to the previous conclusions.

The sentence has been modified to "In summary, the fire aerosols are found to be responsible for up to about half of the total exposures to low visibility in the region."

Line 606: remove "as well"

Removed.

Tables:

Table 2: Please provide more accurate description in the caption. Refer to the TRMM dataset used for observations and mention the different model runs.

This table has been moved to Table 4 and the caption has been modified to "Table 4. The spatial and temporal correlation of monthly rainfall between models (FNL_FINN and

ERA_FINN) and observation (TRMM) during 2003-2014. FMA, MJJ, ASO, NDJ and All represents February-April, May-July, August-October, November-January and whole year, respectively."

Table 3: Please mention that the table includes comparison of different model runs/emissions. Also there are several typos (e.g. "VLD" instead of "LVD"). More details on how the terms in the last column are computed should be provided either in the caption or in the methods. If it is simply the difference from 100% maybe the whole column could be removed. There is an error in the last column FNL_FINN for Bangkok since fire and other pollution contribution appear to be the same.

Typos have been corrected in the revised manuscript. We would like to keep "other pollution contribution" in the table although it is simply the difference from 100%.

Table 2. Annual mean low visibility days (LVDs; observed visibility ≤ 10 km) and very low visibility days (VLVDs; observed visibility ≤ 7 km) per year in Bangkok, Kuala Lumpur, Singapore and Kuching during 2003-2014 are presented in the second column. Parentheses show the percentage of year. The third column shows the percentages, along with standard deviations, of low visibility days explained by fire aerosols alone (i.e. the LVDs captured by the model). The fourth column is the same as the third column but for non-fire (other) pollutions, which is calculated as 100% - fire pollution contribution (i.e. the percentage of LVDs not captured by the model)."

Table 4. Please rephrase the caption. "Annual mean and standard deviation contributed by each source" is not very clear. Line 813 needs to be changed with "Regions s1-s5 are defined in Fig 1.

This table has been moved to Table 3 in the revised manuscript. The caption has been modified to "Table 3. Annual mean and standard deviation of modeled fire $PM_{2.5}$ concentration ($\mu g\ m^{-3}$) in Bangkok, Kuala Lumpur, Singapore, and Kuching during 2003-2014 contributed by each source region (s1 – s5). Parentheses show the percentage of fire $PM_{2.5}$ contribution originating from each source region. Regions s1-s5 are defined in Fig. 1. FNL_FINN, ERA_FINN and FNL_GFED are three model simulations descried in Section 2.1."

Figures

Figure 2: This figure can be still improved. The labels on the x axis should be more frequent and regularly spaced, otherwise it is impossible to infer the months/years of any episode of interest. You could have labels such as mm/yy and regular ticks on the x axis (at least every 6 months or every year). It would be also better to have the same y axis at least for precipitation (0-25) for easier comparison. Although the y-axis for $PM_{2.5}$ cannot be the same for all regions, I am wondering if it is possible to have at least panel b-e on the same scale (0-15) for better comparison and leave panel a up to 40 and mention this in the caption. It would be also easier for the reader to have direct reference the region associated with each panel by adding s1,s2...on top of each panel.

The figure has been modified in the revised manuscript.

Figure 3: rephrase b by simplifying the sentence (e.g. visibility from GSO observations...and FNL_FINN simulations...)

The caption has been modified to "Figure 3. (a) Time series of daily surface $PM_{2.5}$ from the ground-based observations (black line) and FNL_FINN simulated results (red line) in Singapore during 2013-2014. (b) Same as (a) but daily visibility from GSOD observations (black line) and calculated result from FNL_FINN (red line). Highlighted green areas are known haze events caused by fire aerosols, which are reported by news or manually selected based on observed $PM_{2.5}$. Two gray lines mark the visibility of 7 and 10 km, respectively."

Figure 4: Panel 4b is missing, so not sure what line 851 refers to. From "Data points marked with purple" please rephrase. How are those known fire events identified?

4b has been corrected to 3b. The caption has been modified to "Purple points remark the known low visibility events that model failed to produce a visibility at least qualified for LVD." Those known fire events has been described in the caption of Figure 3.

Figure 7: this figure can be improved by placing a frame around each panel and grid lines every month.

The figure has been modified in the revised manuscript.

Figure 9: Panels h to j are not described in the caption. Please add details.

The caption has been modified to "Figure 9. Seasonal mean fire $PM_{2.5}$ concentration (μg m^{-3}) and wind within the PBL modeled in FNL_FINN during February to April, 2003–2014 for fire $PM_{2.5}$ source region from (a) mainland Southeast Asia, (b) Sumatra and Java islands, (c) Borneo, (d) the rest of the Maritime Continent, and (e) northern Australia. (f)-(j) Same as (a)-(e) but for seasonal mean wet scavenging time (days)."

Supplementary Materials:

Figure S2: ERA-Interim is spelled wrong (also in Fig S3)

Corrected.

Figure S5: you should define "A-S-O-F-M-A" in the caption or refer better to the fire seasons.

"F, M and A in the x-axis of (a) indicates February, March and April, respectively. A, S and O in the x-axis of (b) – (d) represents August, September, and October, respectively." has added in the caption of Figure S5 as well as Figure 5.

Figure S6: panels a and b should be improved by placing a frame around each panel and grid lines regularly spaced. Since you are focusing on June-July 2013 the labels could

include just the day and month.

The figure has been modified in the revised manuscript.

Responses to the Comments of the Anonymous Referee #2

We appreciate the additional comments from this reviewer. The following are our point-by-point responses to the reviewer's comments (marked in Italic font). The tracking version of the manuscript is attached with this reply.

The manuscript has been substantially revised. Suggestions for improving the wording in a few places include:
Line 122: add "including" so it becomes "but including dry and wet deposition"
Added.

Line 172 and 177: do the authors mean "anti-correlation" here rather than correlation?
Yes, the word has been corrected.

Line 229: modify to "In general, the model has"
Done.

Line 231: change to "terrain effects" rather than effect
Suggested change has been made.

Line 309: modify to "We first focus"
Done.

Line 312-313: change to "receptor city for the fire events in mainland Southeast Asia"
The change has been made.

Line 318: add "the" so it becomes "to evaluate the model's"
Done.

Line 330: delete "or"
Deleted.

Line 561: change to "fire aerosols over the past decade"
The change has been made.

Line 603: should "exposes" be "exposures" or an equivalent?
Changed to exposures.

Line 604: remove "at"
Done.

Biomass Burning Aerosols and the Low Visibility Events in Southeast Asia

Hsiang-He Lee[1@], Rotem Z Bar-Or[2], and Chien Wang[1,2]

[1] Center for Environmental Sensing and Modeling, Singapore-MIT Alliance for Research and Technology, Singapore

[2] Center for Global Change Science, Massachusetts Institute of Technology, Cambridge, MA, U.S.A.

Submitted to

Atmospheric Chemistry and Physics

June 14, 2016

[@]Corresponding author address: Dr. Hsiang-He Lee, 1 CREATE Way, #09-03 CREATE Tower, Singapore, 138602
E-mail: hsiang-he@smart.mit.edu

Abstract

Fires including peatland burning in Southeast Asia have become a major concern to the general public as well as governments in the region. This is because aerosols emitted from such fires can cause persistent haze events under certain weather conditions in downwind locations, degrading visibility and causing human health issues. In order to improve our understanding of the spatial-temporal coverage and influence of biomass burning aerosols in Southeast Asia, we have used surface visibility and particulate matter concentration observations, supplemented by decadal long (2003 to 2014) simulations using the Weather Research and Forecasting (WRF) model with a fire aerosol module, driven by high-resolution biomass burning emission inventories. We find that in the past decade, fire aerosols are responsible for nearly all the events with very low visibility (< 7km). Fire aerosols alone are also responsible for a substantial fraction of the low visibility events (visibility < 10 km) in the major metropolitan areas of Southeast Asia: up to 39% in Bangkok, 36% in Kuala Lumpur, and 34% in Singapore. Biomass burning in mainland Southeast Asia account for the largest contribution to total fire-produced $PM_{2.5}$ in Bangkok (99%), while biomass burning in Sumatra is a major contributor to fire-produced $PM_{2.5}$ in Kuala Lumpur (50%) and Singapore (41%). To examine the general situation across the region, we have further defined and derived a new integrated metric for 50 cities of the Association of Southeast Asian Nations (ASEAN): ~~i.e., the~~ Haze Exposure ~~Days (HEDs) that~~Day (HED), which measures the annual exposure days of these cities to low visibility (< 10 km) caused by particulate matter pollution. It is shown that HEDs have increased steadily in the past decade across cities with both high and low populations. Fire events alone are found to be responsible for up to about half of the total

HEDs. Our ~~result suggests~~results suggest that in order to improve the overall air quality in Southeast Asia, mitigation policies targeting both biomass burning and fossil fuel burning sources need to be implemented.

1 Introduction

In recent decades, biomass burning has become frequent and ~~widely~~ ~~spread~~widespread across mainland Southeast Asia and the islands of Sumatra and Borneo (Langner et al., 2007; Carlson et al., 2012; Page et al., 2002; van der Werf et al., 2010). Abundant aerosols emitted from such fires cause haze events to occur in downwind locations such as Singapore (Koe et al., 2001; Heil et al., 2007; See et al., 2006), degrading visibility and threatening human health (Emmanuel, 2000; Kunii et al., 2002; Johnston et al., 2012; Mauderly and Chow, 2008; Crippa et al., 2016). Besides causing air quality issues, the fire aerosols contain rich carbonaceous compounds such as black carbon (BC) (Fujii et al., 2014) and thus can reduce sunlight through both absorption and scattering. Indirect effects of fire aerosols on the climate are even more complicated due to various cloud types and meteorological conditions in the Maritime Continent (MC) ~~(Sekiguchi et al., 2003; Lin et al., 2013; Wu et al., 2013).~~(Sekiguchi et al., 2003; Lin et al., 2013; Wu et al., 2013; Grandey et al., 2016).

The majority of present day fires in Southeast Asia occur due to human interference such as land clearing for oil palm plantations, other causes of deforestation, poor peatland management, and burning of agriculture waste (Dennis et al., 2005; Marlier et al., 2015a). Certain policies and regulations, such as those regarding migration, also affect the occurrence of burning events. Large fires have occurred since the 1960s in Sumatra; however, the first fire event in Kalimantan happened in the 1980s (Field et al., 2009). Based on economic incentives and population growth in Southeast Asia, future land-use management will play an important role in determining the occurrence of fires across the region (Carlson et al., 2012; Marlier et al., 2015b).

Besides human interventions, meteorological factors can also influence fire initiation, intensity, and duration (Reid et al., 2012; Reid et al., 2015). Of particular importance is rainfall. Reid et al. (2012) investigated relationships between fire hotspot appearance and various weather phenomena as well as climate variabilities ~~as well as meteorological phenomena~~ in different ~~temporal~~time scales over the MC, including: (1) the El ~~Nino and~~ Niño-Southern Oscillation (ENSO) (Rasmusson and Wallace, 1983; McBride et al., 2003) and the Indian Ocean Dipole (IOD) (Saji et al., 1999); (2) seasonal migration of the Inter-tropical Convergence Zone (ITCZ) and associated Southeast Asia monsoons (Chang et al., 2005); (3) intra-seasonal variability associated with the Madden-Julian Oscillation (MJO) (Madden and Julian, 1971; Zhang, 2005) and the west Sumatran low (Wu and Hsu, 2009); (4) equatorial waves, mesoscale features, and tropical cyclones; and (5) convection. One interesting finding is that the influence of these factors on fire events varies over different parts of the MC. For example, the fire signal in one part of Kalimantan is strongly related to both the monsoons and ENSO. In contrast, fire activity in Central Sumatra is ~~not~~ closely tied to neither the monsoons ~~and~~nor ENSO, but is closely tied to the MJO.

Climate variability of meteorological phenomena affects not only biomass burning emissions but also transport of fire aerosols (Reid et al., 2012). The seasonal migration of the ITCZ and the associated monsoonal circulation dominate seasonal wind flows, whereas sea breezes, tropical cyclones, and topography determine air flow on smaller spatial and temporal scales – all these phenomena play significant roles in determining the transport pathway of fire aerosols (Wang et al., 2013). For example, ~~during~~ the intense haze episode of June 2013, a long lasting event with a “very unhealthy” air

pollution level in Singapore, was actually caused by enhanced fire aerosol transport from Sumatra to West Malaysia owing to a tropical cyclone located in South China Sea. Recently, using a global chemistry transport model combined with a back-trajectory tracer model, Reddington et al. (2014) attempted to attribute particulate pollution in Singapore to different burning sites in surrounding regions over a short time period of 5 years. The coarse 2.8-degree resolution model used in the study, however, has left many open questions.

In this study, we aim to examine and quantify the impact of fire aerosols on the visibility and air quality of Southeast Asia over the past decade. Analyses of observational data and comprehensive regional model results have both been performed in order to improve our understanding of this issue. We firstly describe methodologies adopted in the study, followed by the results and findings from our assessment of the fire aerosol on the degradation of visibility in several selected cities and also over the whole Southeast Asia. We then discuss the sensitivity of our findings to the use of different meteorological datasets as well as fire emission inventories. The last section summarizes and concludes our work.

2 Methodology

2.1 The model

In this study, we have used the Weather Research and Forecasting (WRF) model coupled with a chemistry component (WRF-Chem) version 3.6 (Grell et al., 2005). Our focus in this study is on the fire aerosol life cycle. Therefore, we chose to use WRF-Chem with a modified chemical tracer module instead of a full chemistry package, to

thus model the fire $PM_{2.5}$ particles as tracers without involving much more complicated gaseous and aqueous chemical processing calculations but including dry and wet depositions. Emissions of other chemical species were excluded in the simulations. This configuration lowers the computational burden substantially, and thus allows us to conduct long model integrations to determine the contributions of fire aerosol to the degradation of visibility in the region over the past decade. In WRF-Chem, the sinks of $PM_{2.5}$ particles include dry deposition and wet scavenging calculated at every time step. The simulations are employed within a model domain with a horizontal resolution of 36 km, including 432 × 148 horizontal grid points (Fig. 1), and 31 vertically staggered layers that are stretched to have a higher resolution near the surface (an average depth of ~30 m in the first model half layer) based on a terrain-following pressure coordinate system. The time step is 180 seconds for advection and physics calculation. The physics schemes ~~included~~adopted in the simulations are listed in Table 1. The initial and boundary meteorological conditions are taken from reanalysis meteorological data. In order to examine the potential influence of different reanalysis products on simulation results, we have used two such datasets: (1) the National Center for Environment Prediction FiNaL (NCEP-FNL) reanalysis data (National Centers for Environmental Prediction, 2000), which has a spatial resolution of 1 degree and a temporal resolution of 6 hours; and (2) ERA-Interim, which is a global atmospheric reanalysis from the European Centre for Medium-Range Weather Forecasts (ECMWF) (European Centre for Medium-Range Weather, 2009), providing 6-hourly atmospheric fields on sixty pressure levels from surface to 0.1 hPa with a horizontal resolution of approximately 80 km. Sea surface temperature is updated every 6 hours in both NCEP-FNL and ERA-Interim. All

147 simulations used four-dimensional data assimilation (FDDA) to nudge NCEP-FNL or
148 ERA-Interim temperature, water vapor, and zonal as well as meridional wind speeds
149 above the planetary boundary layer (PBL). This approach has been shown to provide
150 realistic temperature, moisture, and wind fields in a long simulation (Stauffer and
151 Seaman, 1994).

152 Two biomass burning emission inventories are also used in this study to investigate
153 the sensitivity of modeled fire aerosol concentration to different emission estimates. The
154 first emission inventory is the Fire INventory from NCAR version 1.5 (FINNv1.5)
155 (Wiedinmyer et al., 2011), which classifies burnings of extra tropical forest, tropical
156 forest (including peatland), savanna, and grassland. It is used in this study to provide
157 daily, 36 km resolution $PM_{2.5}$ emissions. The second emission inventory is the Global
158 Fire Emission Database version 4.1 with small fires included (GFEDv4.1s) (van der Werf
159 et al., 2010; Randerson et al., 2012; Giglio et al., 2013). GFEDv4.1s provides $PM_{2.5}$
160 emissions with the same spatiotemporal resolution as FINNv1.5.

161 Our simulations cover a time period slightly longer than a decade from 2003 to 2014
162 based on available biomass burning emission estimates. The simulation of each year
163 started on 1 November of the previous year and lasted for 14 months. The first two
164 months were used for spin-up.

165 Three sets of decadal long simulations have been conducted. The first simulation
166 used NCEP-FNL reanalysis data and the FINNv1.5 fire emission inventory. This
167 simulation is hereafter referred to as FNL_FINN and is discussed as the base simulation.
168 In order to examine the influence of different meteorological inputs on fire aerosol life
169 cycle, the second simulation was conducted using the same FINNv1.5 fire emission

inventory as in FNL_FINN but different reanalysis dataset, the ERA-Interim, and is referred to as ERA_FINN. In addition, to investigate the variability of fire aerosol concentration brought by the use of different estimates of fire emissions, the third simulation, FNL_GFED, was driven by the same NCEP-FNL meteorological input as in FNL_FINN but with a different fire emission inventory, the GFEDv4.1s.

A plume rise algorithm for fire emissions was implemented in WRF-Chem by Grell et al. (2011) to estimate fire injection height. This algorithm, however, often derives an injection height for tropical peat fire that is too high compared to the estimated value based on remote sensing retrievals (Tosca et al., 2011). Therefore, we have limited the plume injection height of peat fire by a ceiling of 700 m above the ground in this study based on Tosca et al. (2011). The vertical distribution of emitted aerosols is calculated using the plume model. This modification has clearly improved the modeled surface $PM_{2.5}$ concentration when compared to observations in Singapore.

In order to distinguish the spatial-temporal coverage and influence of biomass burning aerosols from different regions in Southeast Asia and nearby northern Australia, we have created five tracers to represent fire aerosols respectively from mainland Southeast Asia (s1), Sumatra and Java islands (s2), Borneo (s3), the rest of the Maritime Continent (s4), and northern Australia (s5) as illustrated in Fig. 1. ~~The major~~Based on this design, we are able to identify fire ~~season in mainland Southeast Asia (s1) is~~$PM_{2.5}$ concentration from ~~February to April. In the other four~~different regions ~~(s2-s5), it is from August~~and estimate the contribution to ~~October.~~the total fire $PM_{2.5}$ in a receptor city.

Generally speaking, ~~there~~the major fire season in mainland Southeast Asia (s1) is from February to April and in the other four regions (s2-s5), it is from August to October.

There is a strong anti-correlation between the seasonal variation of fire emissions and that of rainfall in all fire regions as shown in Fig. 2. Because mainland Southeast Asia (s1) and northern Australia (s5) are on the edge of the seasonal migration of the ITCZ, the correlation in these two regions is even more pronounced. On the other hand, ~~in~~ Sumatra (s2), Borneo (s3) and the rest of the Maritime Continent (s4~~), while inter-seasonal variations of rainfall and fire emissions are still correlated with each other in general, however, fire emissions~~) do ~~exist in some raining~~not have clearly identifiable dry seasons and this contributes to the weaker correlation (Fig. 2b – d~~), owing to the precipitation features in multiple scales over these regions (e.g., the passage of MJO events) and~~). Besides that, underground peatland burning~~ –~~ may not be immediately extinguished by precipitation.

~~2.2 Numerical simulations and model evaluation~~

~~Our simulations cover a time period slightly longer than a decade from 2003 to 2014 based on available biomass burning emission estimates. The simulation of each year started on 1 November of the previous year and lasted for 14 months. The first two months were used for spin-up.~~

~~Three sets of decadal-long simulations have been conducted. The first simulation used NCEP-FNL reanalysis data and the FINNv1.5 fire emission inventory. This simulation is hereafter referred to as FNL_FINN and is discussed as the base simulation. In order to examine the influence of different meteorological inputs on fire aerosol life cycle, the second simulation was conducted using the same FINNv1.5 fire emission inventory as in FNL_FINN but different reanalysis dataset, the ERA-Interim, and is referred to as ERA_FINN. In addition, to investigate the variability of fire aerosol~~

~~concentration brought by the use of different estimates of fire emissions, the third simulation, FNL_GFED, was driven by the same NCEP-FNL meteorological input as in FNL_FINN but with a different fire emission inventory, the GFEDv4.1s. Note that the simulation period from 2003 to 2014 of all these simulations was solely decided based on the temporal coverage of GFEDv4.1s.~~

~~Precipitation and wind are two key factors in determining the transport and scavenging of fire aerosols. They are also the variables we use to evaluate the model's performance in simulating meteorological features. The WRF simulation driven by NCEP-FNL reanalysis data, the FNL_FINN run, produced a monthly mean precipitation of 6.80±0.55 mm day^{-1} over the modeled domain for the period from 2003 to 2014, very close to the value of 6.30±0.43 mm day^{-1} produced in another simulation driven by ERA-Interim, the ERA_FINN run. However, the average rainfall in both runs appears to be higher than the monthly mean of 4.71±0.37 mm day^{-1} from the satellite-retrieved precipitation of the Tropical Rainfall Measuring Mission (TRMM) 3B43 (V7) dataset (Huffman et al., 2007). Based on the sensitivity tests for FDDA grid nudging, the wet bias in both experiments mainly comes from water vapor nudging. Figure S1a – c are the Hovmöller plots of daily TRMM, FNL_FINN, and ERA_FINN precipitation in 2006, respectively. Compared to the satellite-retrieved data, both FNL_FINN and ERA_FINN have produced more light rain events, and this appears to be the reason behind the model precipitation bias. Despite the model overestimate in average total precipitation, the temporal correlation of monthly rainfall between FNL_FINN and TRMM is 0.68 and the spatial correlation is 0.85 during 2003-2014 (Table 2). For ERA_FINN, the temporal correlation with TRMM is 0.90, while the spatial correlation is 0.85. In the summer~~

~~monsoon season (i.e., May, June and July), both runs show the highest temporal correlations with observation but the lowest in the spatial correlations. The comparisons show that simulated rainfall generally agrees with the observation in space and time, especially when ERA-Interim reanalysis is used (i.e., in ERA_FINN).~~

~~The representative wind pattern in Southeast Asia is the monsoon wind flow. In the winter monsoon season (i.e., February, March and April), mean surface winds are from northeast in the Northern Hemisphere and turn to the northwesterly once past the Equator (Fig. S2a). On the other hand, the wind directions are reversed in the summer monsoon season (i.e., August, September and October) (Fig. S2b). We use the wind data from NCEP-FNL and ERA-Interim reanalysis to evaluate model simulated winds. We find that both runs overestimated the u component (stronger easterly) in South China Sea (Fig. S3a and c) in the winter monsoon season, and overestimated the v component (stronger southerly) in Java Sea in the summer monsoon season (Fig. S3b and d). These regions are the entrances of monsoon wind flow into the MC. In general, model has well captured the general wind flows in Southeast Asia during both monsoon seasons but overestimated about 1 m sec^{-1} in wind speed in some regions likely due to terrain effect and model resolution limitation.~~

~~2.3~~2.2 Observational data and model derivation of visibility

The definition of "visibility" is the farthest distance at which one can see a large, black object against a bright background at the horizon (Seinfeld and Pandis, 2006). There are several factors determining visibility, but here we mainly consider the absorption and scattering of light by gases and aerosol particles, excluding fog or misty

days. In this study, the modeled visibility is calculated by using the *Koschmeider equation*:

$$VIS = 3.912 / b_{ext}, \quad (1)$$

where *VIS* is visibility with a unit in meter and b_{ext} is the extinction coefficient with a unit of m^{-1}. Excluding fog, visibility degradation is most readily observed from the impact of particulate pollution. Based on Eq. (1), a maximum visibility under an absolutely dry and pollution-free air is about 296 km owing to Rayleigh scattering, while a visibility in the order of 10 km is considered ~~under a~~indicative of moderate to heavy air pollution by particulate matter (Visscher, 2013). Abnormal and persistent low visibility situations are also referred to as "haze" events. Air pollution sources such as fossil fuel burning, can cause low visibility and haze events to occur. Similarly, fire aerosols, alone or mixed with other particulate pollutants, can degrade visibility by increasing b_{ext} and lead to occurrence of haze events too.

The observational data of visibility from the Global Surface Summary of the Day (GSOD) (Smith et al., 2011) are used in our study to identify days under particulate pollution, i.e., haze events. The GSOD is derived from the Integrated Surface Hourly (ISH) dataset and archived at the National Climatic Data Center (NCDC). The daily visibility in the dataset is available from 1973 to the present.

The observed visibility is also used to evaluate the modeled visibility and thus $PM_{2.5}$ concentration. The modeled visibility is derived based on the extinction coefficient of the fire aerosols as a function of particle size, by assuming a log-normal size distribution of accumulation mode with a standard deviation $\sigma = 2$ (Kim et al., 2008). Note that all these calculations are done for the wavelength of 550 nm unless otherwise indicated. As

fire plumes contain both sulfur compounds and carbonaceous aerosols, we assume the fire aerosols are aged internal mixtures with black carbon as the core and sulfate as the shell (Kim et al., 2008). To make the calculated visibility of the fire aerosols better match the reality, we have also considered hydroscopic growth of sulfate fraction of these mixed particles in the calculation based on the modeled relative humidity (*RH*). Based on Kiehl et al. (2000), the hydroscopic growth factor (*rhf*) is given by

$$rhf = 1.0 + exp(a_1 + \frac{a_2}{RH+a_3} + \frac{a_4}{RH+a_5}), \quad (2)$$

where a_1 to a_5 are fitting coefficients given by 0.5532, -0.1034, -1.05, -1.957, 0.3406, respectively. The radius increase of wet particle (r_{wet}) due to hydroscopic growth will be

$$r_{wet} = {r_{dry}}^{rhf}, \quad (3)$$

where r_{dry} is the radius of dry particle in micron.

As mentioned above, a visibility of 10 km is considered an indicator ~~for a~~of moderate to heavy particulate pollution. Hence ~~a~~an observed visibility of 10km ~~in observation~~ is used as the threshold for defining the "low visibility day (VLD)" in our study. We firstly derived the observed low visibility days in every year for a given city using the GSOD visibility data. Then, we derived the modeled low visibility days following the same procedure but using modeled visibility data that were only influenced by fire aerosols. Both the observed and modeled visibilities were then used to define the fraction of low visibility days that can be ~~caused~~explained by fire aerosols alone. It is assumed that whenever fire aerosol *alone* could cause a low visibility day to occur, such a day would be attributed to fire aerosol caused LVD, regardless of whether other coexisting pollutants would have a sufficient intensity to cause low visibility or not. In addition to the LVD, we have also used a daily visibility of 7 km as the criterion to define

the observed "very low visibility day (VLVD)". Such heavy haze events in the region are generally caused by severe fire aerosol pollution, thus we use their occurrence specifically to evaluate the model performance.

~~2.4~~2.3 The "Haze Exposure Day (HED)"

We have derived a metric, the Haze Exposure Day (HED), to measure the exposure of the whole Southeast Asia, represented by 50 cities of the Association of Southeast Asian Nations (ASEAN), to low visibility events. HED can be defined in a population weighted format for the analyzed 50 cities, indicating the relative exposure of the populations in these cities to the low visibility events caused by particulate pollution:

$$HED_{pw} = \sum_{i=1}^{N} C_{pw}(i), \quad (4)$$

where,

$$C_{pw}(i) = pop(i) \cdot C(i) / \sum_{i=1}^{N} pop(i), \quad (5)$$

is the population-weighted fraction of the total Haze Exposure Days, *N* equals to the total number of cities (50), *i* is the index for the 50 analyzed cities, *pop(i)* is the population for a given city (Table S1), and *C(i)* represents the annual LVDs for that city calculated from the GSOD dataset. Note that we assume that the population of each city stays constant throughout the analyzed period. Another assumption of HED_{pw} is that everyone in a given city would be equally exposed to the particulate pollution.

In addition, HED can be also defined in an arithmetic mean format, assuming each city weights equally regardless of its population. Its value hence emphasizes on the relative exposure of each area within the analyzed region:

$$HED_{ar} = \sum_{i=1}^{N} C(i)/N. \quad (6)$$

Both HED_{pw} and HED_{ar} can be also calculated using fire-caused LVDs to define the absolute and relative contributions of fire aerosols to the total low visibility events in the region. We will label the fire-caused HED as $fHED_{pw}$ and $fHED_{ar}$ ~~thereafter~~.

3 Assessment of the impact of fire aerosols on the visibility in Southeast Asia

3.1 Impact of fire aerosols on the visibility in four selected cities

We first to focus our analysis on four selected cities in the region, Bangkok (Thailand), Kuala Lumpur (Malaysia), Singapore (Singapore), and Kuching (Malaysia), all located close to the major fire sites ranging from the mainland to the islands of Southeast Asia. Specifically, Bangkok is a smoke receptor city ~~of~~for the fire events in mainland of Southeast Asia (s1) while Kuala Lumpur and Singapore are two cities frequently under the influence of Sumatra (s2) as well as Borneo fires (s3). Kuching is in the coastal area of Borneo and directly affected by Borneo fire events (s3).

The surface observational data of $PM_{2.5}$ concentration among these four cities are only available in Singapore since 2013 from the National Environment Agency (NEA) of Singapore. We thus firstly used these data along with visibility data to evaluate the model's performance for fire-caused haze events reported in Singapore during 2013-2014 (Fig. 3). Note that the observed $PM_{2.5}$ level reflects the influences of both fire and non-fire aerosols, whereas the modeled $PM_{2.5}$ only includes the impact of fire aerosols. We find that the model still predicted clearly high $PM_{2.5}$ concentrations during most of the observed haze events, especially in June 2013, and in spring and fall seasons of 2014 ~~(highlighted green areas),~~ though with underestimates in particle concentration of up to 30-50%, likely due to the model's exclusion of non-fire aerosols, coarse model

resolution, overestimated rainfall, or errors in the emission inventory. Figure 4 shows observed visibility versus modeled visibility in FNL_FINN during the fire events shown in Fig. 3. Note that all these events have an observed visibility lower than or equal to 10 km, or can be identified as LVDs. In capturing these fire-caused haze events, the model only missed about 22% of them, ~~or~~ reporting a visibility larger than 10 km in 40 out of 185 observed LVDs as marked with purple color in Fig. 4. When observed visibility is between 7 and 10 km, model results appear to align with observations rather well. For cases with visibility lower than 7 km, the model captured all the events (by reporting a visibility lower than 10 km, or LVD) although often overestimated the visibility range. These results imply that the VLVDs only count a very small fraction in LVDs and thus are episodic events. It is very likely that the size of concentrated fire plumes in VLVDs might be constantly smaller than the 36 km model resolution; therefore, the model results could not reach the peak values of $PM_{2.5}$ concentrations of these plumes.

Furthermore, the LVDs in the four selected near-fire-site cities during the fire seasons from 2003 to 2014 have been identified using the daily GSOD visibility database and then compared with modeled results (Fig. 5). It is difficult to identify all the fire caused haze events beyond Singapore even in recent years. However, in Southeast Asia, severe haze events equivalent to the VLVDs in visibility degradation are known to be largely caused by fire aerosol pollution. Therefore, we used the observed VLVDs in the four selected cities to evaluate the performance of the model. We find that the modeled result displays a good performance in capturing VLVDs despite an overestimate in visibility range during certain events compared with the observation. The model in general only missed about 10% or fewer VLVDs observed in the past decade (Table ~~3~~2;

Fig. 5). In addition, the model has reasonably captured the observed LVDs despite certain biases (Fig. 5), likely due to the fact that fire aerosol might not be the only reason responsible for the degradation of visibility during many LVDs.

We find that the annual mean LVDs in Bangkok has increased from 47% (172 days) in the first 5-year period of the simulation duration (2003-2007) to 74% (272 days) in the last 5-year period (2010-2014). The LVDs caused by fire aerosols has increased as well (Fig. 6a). Overall, fire aerosols are responsible for more than one third of these LVDs (i.e., 39% in average; Table ~~3~~2). The largest source of fire aerosols affecting Bangkok is burning of agriculture waste and other biomass in s1 during the dry season of spring (Fig. 7a; Table ~~4~~3). During the fire season, abundant fire aerosols degrade visibility and even cause VLVDs to occur, mainly from December to April (Fig. 6e). Based on our model results, 87% of VLVDs can be identified as ~~fire~~ caused by fires.

In Kuala Lumpur, the percentage of LVDs also gradually increases since 2006 to reach a peak in 2011 and again in 2014 (Fig. 6b). During 2005-2010 the frequency of total LVDs have increased 10-15% each year, mainly attributing to the pollution sources other than fires. However, fire-caused LVDs become more evident after 2009. Seasonal wise, there are two peaks of fire aerosol influence, one in February-March and another in August (Fig. 6f), corresponding to the trans-boundary transport of fire aerosols from mainland Southeast Asia (s1) in the winter monsoon season and from Sumatra (s2) in the summer monsoon season, respectively (Fig. 7b). Three quarter of VLVDs occurred in the summer monsoon season due to Sumatra fires. Note that in November and December the percentage of LVDs is over 50% and dominated by pollutants other than fire aerosols. These non-fire aerosols presumably come from either local sources or the areas further

inland riding on the winter monsoon circulation. Overall, fire pollution is responsible for 36%, a substantial fraction of total low visibility events in Kuala Lumpur during 2003-2014 (Table ~~3~~2).

The percentage of LVDs in Singapore has been rapidly increasing since 2012 (Fig. 6c). During the simulation period, this increase appears to be mostly from anthropogenic pollution other than fires, especially in 2012 and 2013. In monthly variation, ~~similar~~similarly to Kuala Lumpur, two peaks of fire aerosol influence appear in February-March and in September-October, respectively (Fig. 6g). In February and March, the trans-boundary transport of fire aerosols come from mainland Southeast Asia (s1), while in the summer monsoon season fire aerosols come from both Sumatra (s2) and Borneo (s3) (Fig. 7c). Except for the severe haze events in June 2013, VLVDs basically occur in September and October (i.e., 92%) due to both Sumatra and Borneo fires. In general, up to 34% of LVDs in Singapore are caused by fire aerosols based on the FNL_FINN simulation and the rest by local and long-range transported pollutants (Table ~~3~~2). Nevertheless, fire aerosol is still the major reason for the episodic severe haze conditions.

Because of its geographic location, Kuching is affected heavily by local fire events during the fire season (Fig. 7d). Fire aerosols can often degrade the visibility to below 7 km and even reaching 2 km (Fig. 5d). The LVDs mainly occur in August and September during the fire season (Fig. 6d and h). The frequency of LVDs in Kuching is ~~similar~~similarly to Singapore; however, 25% of those LVDs are considered to be VLVDs in Kuching while only 4% are in Singapore in comparison (Table ~~3~~2).

3.2 Impact of fire aerosols on the visibility over the whole Southeast Asia

Air quality degradation caused by fires apparently occurs in regions beyond the above-analyzed four cities. To examine such degradation over the whole Southeast Asia, we have extended our analysis to cover 50 cities of the ASEAN. The impact of particulate pollution on the whole Southeast Asia is measured by the "Haze Exposure Day" (HED) as defined in Section 2.~~5~~3. The top four among the 50 cities that made the largest contributions to the HED_{pw} are Jakarta, Bangkok, Hanoi, and Yangon (Fig. 8a), with population ranking of 1, 2, 4, and 5, respectively (Table S1).

We find that both HED_{pw} and HED_{ar} increase rather steadily over the past decade (Fig. 8b), demonstrating that the exposure to haze events either weighted by population or not has become worse in the region. Generally speaking, the fire aerosols are responsible for up to 40-60% of the total exposure to low visibility across the region. In both measures, the increase of fire-caused HED (2.64 and 3.37 days per year for population-weighted and arithmetic mean, respectively) is ~~similar~~similarly to that of overall HED (2.61 and 3.59 days per year for population-weighted and arithmetic mean, respectively) (Fig. 8b), suggesting that fire aerosol has taken the major role in ~~causing the degradation of~~degrading air quality in Southeast Asia compared to the non-fire particulate pollution. The result that HED_{pw} is higher than HED_{ar} in most of the years indicates that the particulate pollution is on average worse over more populous cities than the others. Interestingly, the discrepancy of these two variables, however, has become smaller in recent years and even reversed in 2014, implying an ~~equally worsening~~increase of haze ~~event~~ occurrence across ~~from the smaller to bigger~~ cities ~~in terms of population~~with different populations in the region. The reason behind this could be a

441 wider spread of fire events in the region, causing acute haze events in cities even with
442 relatively low populations. Regarding the increase of fire-caused HED, because biomass
443 burning, especially peatland burning, usually occurs in the rural areas, higher fire
444 emissions would extend low visibility conditions to a larger area regardless of its
445 population. On the other hand, due to industrialization, urbanization, and other factors
446 such as population growth, air pollution has become worse across the region so even
447 cities with lower populations now increasingly suffer from low visibility from fossil fuel
448 burning and other sources of particulate pollution (IEA, 2015). Therefore, the mitigation
449 of air quality degradation needs to consider both fire and non-fire sources.

450 **3.3 The influence of wind and precipitation on fire aerosol life cycle**

451 Seasonal migrations of the ITCZ and associated summer and winter monsoons
452 dominate seasonal wind flows that drive fire aerosol transport. Additionally, as discussed
453 previously, certain small-scale or short-term phenomena such as sea breezes, typhoons,
454 and topography-forced circulations also play important roles in distributing fire aerosols.
455 Nevertheless, we focus our discussion here on the former.

456 From February to April is the main fire season in mainland Southeast Asia (s1). In
457 the FNL_FINN simulation, the seasonal mean concentration of $PM_{2.5}$ within the PBL can
458 exceed 20 μg m^{-3} in this region (note that the air quality standard suggested by World
459 Health Origination is 10 μg m^{-3} for annual mean and 25 μg m^{-3} for 24-h mean). During
460 this fire season, the most common wind direction is from northeast to southwest across
461 the region (Fig. 9a). Fire aerosol plumes with concentrations higher than 0.1 μg m^{-3} can
462 be transported westward as far as 7000 km from the burning sites (Fig. 9a). In contrast,
463 February to April is not the typical burning season in the islands. Low fire emissions in

combination with a lack of long-range transport of fire aerosols from the mainland due to the seasonal circulation result in a low $PM_{2.5}$ level over these regions (Fig. 9b - d).

Wet scavenging is a major factor determining the lifetime and thus abundance of suspended fire aerosols in the air. The effect of wet scavenging of fire aerosols is reflected from the wet scavenging time calculated using the modeled results, which is a ratio of the aerosol mass concentration to the scavenging rate (a function of precipitation rate). Thus, short scavenging times often indicate high scavenging rates except for the sites with extremely low aerosol concentration. During February-April, at the ITCZ's furthest southern extent, the short scavenging time < 1 day around 10°S shows a quick removal of fire aerosols by heavy precipitation, preventing the southward transport of aerosols (Fig. 9f). On the other hand, the long scavenging time (> 5 days) in the Western Pacific warm pool, South China Sea, the Indochina peninsula, Bay of Bengal, and Arabian Sea leads to a long suspending time of aerosols transported to these regions. During the same season, over the islands of Sumatra and Borneo, the abundance of fire aerosols, either emitted locally or trans-boundary transported, are greatly limited by the high scavenging rate (short scavenging time) over these regions (Fig. 9g and h). The South China Sea has little precipitation during this time period; therefore, fire aerosols from the northern part of the Philippines can be transported to this region and stay longer than 5 days (Fig. 9i).

The months of August to October, when the ITCZ reaches its furthest northern extent, mark the major fire season of Sumatra, Borneo, and some other islands in the MC (Fig. ~~S5b~~S1b - d). Australia fires also mainly occur in this season (Fig. ~~S5e~~S1e). Mean wind flows are from southeast to northwest in the Southern Hemisphere, and turn to the

487 northeast direction once past the Equator. Within the MC the seasonal variation of
488 rainfall is small during this time, with heavy precipitation and thus short scavenging
489 times (< 3 days) existing along the MJO path (Fig. ~~S5f~~S1f - i) (Wu and Hsu, 2009). The
490 high scavenging rate in the regions close to the fire sites in the islands shortens the
491 transport distance of fire aerosol plumes with $PM_{2.5}$ concentration > 0.1 μg m^{-3} to less
492 than 3000 km (Fig. ~~S5b~~S1b - d). Long scavenging times (> 5 days) exist in the Banda
493 Sea and northern Australia due to the ITCZ location. Fire aerosols from Java (s2) (Fig.
494 ~~S5g~~S1g), Papua New Guinea (s4) (Fig. ~~S5i~~S1i), and northern Australia (s5) (Fig. ~~S5j~~S1j)
495 can thus be suspended in the air for a relatively long time over these regions.

496 The above-discussed seasonal features of precipitation and aerosol scavenging
497 rate help us to better understand the variability of haze occurrence and also to
498 identify the major source regions of fire aerosols influencing selected Southeast
499 Asian cities (Fig. 7). For example, the geographic location of Bangkok, which is
500 inside the s1 emission region, determines that nearly all the fire aerosols (99%) are
501 from sources within the region from December to April (Fig. 7a and Table ~~4~~3). Fire
502 aerosols from all the other burning sites stay at very low levels even during the
503 burning seasons there due to circulation and precipitation scavenging. For Kuala
504 Lumpur and Singapore, over 90% of the fire aerosols reaching both cities come from
505 mainland Southeast Asia (s1) in January–April due to the dominant winter monsoon
506 circulation. During May-October, however, the major sources of fire aerosols shift to
507 Sumatra (s2) and Borneo (s3) aided by northward wind (Fig. ~~S5b~~S1b and c). The
508 monthly variations of $PM_{2.5}$ concentration in Kuala Lumpur and Singapore also have
509 a largely similar pattern (Fig. 7b and ~~d~~c). The annual mean contribution of different

emission regions in Kuala Lumpur are 43% from mainland Southeast Asia (s1), 50% from Sumatra (s2), 4% from Borneo (s3), 3% from the rest of Maritime Continent (s4), and 0.3% from northern Australia (s5) in FINL_FINN (Table ~~4). Similar~~3). Similarly to Kuala Lumpur, there are two peak seasons of the monthly low visibility days contributed by fire aerosols in Singapore (Fig. 6g), well correlated with modeled high fire $PM_{2.5}$ concentration (Fig. 7c). The low visibility days in March and April mainly are caused by fire aerosols from mainland Southeast Asia (s1) under southward wind pattern (Fig. 9a), and those in May to October are affected by Sumatra (s2) first in May to June, and then by both s2 and s3 (Borneo) during August to October due to north- or northwest-ward monsoonal circulation (Fig. ~~S5b~~S1b and c; also Table 43). Kuching, ~~similar~~similarly to Bangkok, is strongly affected by local fire aerosols (s3) during the fire season (July – October). The annual mean contribution from Borneo (s3) is 85%, with only 8% from mainland Southeast Asia (s1) and 5% from Sumatra (s2) (Table 43).

~~Reddington et al. (2014) applied two different models, a 3D global chemical transport model and a Lagrangian tracer model to examine the long-term mean contributions of fire emissions from different regions to $PM_{2.5}$ in several cities in Southeast Asia. Their estimated contribution from mainland Southeast Asia to the above-discussed four selected cities was lower than our result during January-May, likely due to their use of a different emission inventory and the coarse resolution of their global model. The FINNv1.5 dataset used in our study specifically provides higher $PM_{2.5}$ emissions from agriculture fires (the major fire type in mainland Southeast Asia) than GFED4.1s does – the latter is an updated version of the dataset (GFEDv3) used in Reddington et al.~~

~~(2014) (Fig. 2). The detailed comparison of FNL_FINN and FNL_GFED will be discussed in the following section.~~

4 Influence of different meteorological datasets and emission inventories on modeled fire aerosol abundance

4.1 Different meteorological datasets

Meteorological conditions, particularly wind fields and precipitation, could substantially influence the life cycle and transport path of fire aerosols during the fire seasons. First of all, we use these two variables to evaluate the model's performance in simulating meteorological features. The WRF simulation driven by NCEP-FNL reanalysis data, the FNL_FINN run, produced a monthly mean precipitation of 6.80±0.55 mm day^{-1} over the modeled domain for the period from 2003 to 2014, very close to the value of 6.30±0.43 mm day^{-1} produced in another simulation driven by ERA-Interim, the ERA_FINN run. However, the average rainfall in both runs appears to be higher than the monthly mean of 4.71±0.37 mm day^{-1} from the satellite-retrieved precipitation of the Tropical Rainfall Measuring Mission (TRMM) 3B43 (V7) dataset (Huffman et al., 2007). Based on the sensitivity tests for FDDA grid nudging, the wet bias in both experiments mainly comes from water vapor nudging. Figure S2a – c are the Hovmöller plots of daily TRMM, FNL_FINN, and ERA_FINN precipitation in 2006, respectively. Compared to the satellite-retrieved data, both FNL_FINN and ERA_FINN have produced more light rain events, and this appears to be the reason behind the model precipitation bias. Despite the model overestimate in average total precipitation, the temporal correlation of monthly rainfall between FNL_FINN and TRMM is 0.68 and the spatial correlation is

0.85 during 2003-2014 (Table 2). For ERA_FINN, the temporal correlation with TRMM is 0.90, while the spatial correlation is 0.85. In the summer monsoon season (i.e., May, June and July), both runs show the highest temporal correlations with observation but the lowest in the spatial correlations. The comparisons show that simulated rainfall generally agrees with the observation in space and time, especially when ERA-Interim reanalysis is used (i.e., in ERA_FINN).

The representative wind pattern in Southeast Asia is the monsoon wind flow. In the winter monsoon season (i.e., February, March and April), mean surface winds are from northeast in the Northern Hemisphere and turn to the northwesterly once past the Equator (Fig. ~~As discussed in the previous section, meteorological conditions, particularly wind field and precipitation, could substantially influence the life cycle and transport path of fire aerosols during the fire seasons. Therefore, it is necessary to examine potential discrepancy in modeled particulate matter abundance arising from the use of different meteorological datasets.~~

~~When comparing two of our simulations, one driven by the NCEP-FNL (i.e., FNL_FINN) and the other by the ERA-Interim (i.e., ERA_FINN) meteorological input~~S3a). On the other hand, the wind directions are reversed in the summer monsoon season (i.e., August, September and October) (Fig. S3b). We use the wind data from NCEP-FNL and ERA-Interim reanalysis to evaluate model simulated winds. We find that both runs overestimated the u component (stronger easterly) in South China Sea (Fig. S4a and c) in the winter monsoon season, and overestimated the v component (stronger southerly) in Java Sea in the summer monsoon season (Fig. S4b and d). These regions are the entrances of monsoon wind flow into the MC. In general, the model has well

captured the general wind flows in Southeast Asia during both monsoon seasons but overestimated about 1 m s^{-1} in wind speed in some regions likely due to terrain effect and model resolution limitation.

When comparing two of our simulations, FNL_FINN and ERA_FINN, we find that the ERA_FINN run consistently produces less precipitation than the FNL_FINN run during the rainy seasons over the past decade (Fig. ~~2; also see the comparison results of both runs with observations in Section 2.2.).~~2). Regarding fire aerosol life cycle, less rainfall in ERA_FINN results in weaker wet scavenging and thus higher abundance of fire aerosols than in FNL_FINN. We find that the annual mean concentration of fire $PM_{2.5}$ produced in the ERA_FINN run in Bangkok, Kuala Lumpur, Singapore, and Kuching is 9.2, 5.8, 3.4, and 7.7 μg m^{-3}, respectively, clearly higher than the corresponding results of the FNL_FINN run of 8.5, 5.3, 3.0, and 6.9 μg m^{-3} (Table 43). In general, fire $PM_{2.5}$ concentration in ERA_FINN is about 10% higher than in FNL_FINN. However, the occurrence of low visibility events is less sensitive to the differences in rainfall in places near the burning areas such as Bangkok and Kuching, as indicated by a nearly negligible enhancement of VLVDs in the ERA_FINN run in Bangkok and Kuching (~1%) (Table ~~3~~2). In comparison, the difference in wind ~~field~~fields between the two runs has a much smaller impact than that of precipitation on modeled particulate matter abundance.

4.2 Different biomass burning emission inventories

In addition to meteorological inputs, using different fire emission estimates could also affect the modeled ~~results.~~$PM_{2.5}$ concentration. To examine ~~such an influence~~this impact, we have compared two simulations with the same meteorological input but

601 different fire emission inventories, the FNL_FINN using FINNv1.5 and FNL_GFED
602 using GFEDv4.1s. The main differences between the two emission inventories appear
603 mostly in mainland Southeast Asia (s1) and northern Australia (s5) (Fig. 2a and e).
604 Compared to FINNv1.5, fire emissions in GFEDv4.1s over mainland Southeast Asia are
605 more than 66% lower (Fig. 2a), and this results in a 43% lower fire $PM_{2.5}$ concentration in
606 Bangkok (Table 43). The lower fire $PM_{2.5}$ concentration in FNL_GFED actually
607 produces a visibility that matches better with observations in Bangkok comparing to the
608 result of FNL_FINN (Fig. S5a). This implies that the fire emissions in FINNv1.5 are
609 perhaps overestimated in mainland Southeast Asia. In northern Australia, fire aerosol
610 emissions suggested by FINNv1.5 are almost negligible compared to GFEDv4.1s (Fig.
611 2e). Therefore, in the FNL_GFED simulation, Australia fire aerosols play an important
612 role in Singapore air quality, contributing to about 22% of the modeled $PM_{2.5}$
613 concentration in Singapore. In contrast, Australia fires have nearly no effect on
614 Singapore air quality in the FNL_FINN run (Table 43).

615 We would also like to point out the importance of spatiotemporal distribution of fire
616 emission to the modeled ~~results.~~ $PM_{2.5}$ concentration. For example, during the June 2013
617 severe haze event in Kuala Lumpur and Singapore, the total amount of fire emissions
618 from Sumatra (s2) in GFEDv4.1s are lower than those of FINNv1.5 (Fig. S6a) but
619 distributed rather more densely over a smaller area (Fig. S6c and d). As a result, under
620 the same meteorological conditions, the simulated $PM_{2.5}$ in the FNL_GFED simulation
621 reaches Singapore in a higher concentration that also matches better with observations
622 than the result of FNL_FINN (Fig. ~~S7b~~S6b).

Reddington et al. (2014) applied two different models, a 3D global chemical transport model and a Lagrangian tracer model to examine the long-term mean contributions of fire emissions from different regions to $PM_{2.5}$ in several cities in Southeast Asia. Their estimated contribution from mainland Southeast Asia to the above-discussed four selected cities in Section 3.1 was lower than our result during January-May, likely due to their use of a different emission inventory and the coarse resolution of their global model. The FINNv1.5 dataset used in our study specifically provides higher $PM_{2.5}$ emissions from agriculture fires (the major fire type in mainland Southeast Asia) than GFED4.1s does – the latter is an updated version of the dataset (GFEDv3) used in Reddington et al. (2014) (Fig. 2).

5 Summary and Conclusions

We have examined the extent of the biomass burning aerosol's impact on the air quality of Southeast Asia ~~in~~over the past decade using surface visibility and $PM_{2.5}$ measurements along with the WRF model with a modified fire tracer module. The model has shown a good performance in capturing 90% of the observed severe haze events (visibility < 7 km) caused by fire aerosols occurred over the past decade in several cities that are close to the major burning sites. Our study also suggests that fire aerosols are responsible for a substantial fraction of the low visibility days (visibility < 10 km) in these cities: up to 39% in Bangkok, 36% in Kuala Lumpur, 34% in Singapore, and 33% in Kuching.

In attributing the low visibility events to fire emissions from different sites, we find that mainland Southeast Asia is the major contributor during the ~~Northeast~~northeast or winter monsoon season in Southeast Asia. In the ~~Southwest~~southwest or summer

monsoon season, however, most fire aerosols come from Sumatra and Borneo. Specifically, fires in mainland Southeast Asia ~~are accounted~~account for the largest percentage of the total fire $PM_{2.5}$ in Bangkok (99%), and fires from Sumatra are the major contributor in Kuala Lumpur (50%) and Singapore (41%). Kuching receives 85% of fire aerosols from local Borneo fires.

By comparing the results from two modeled runs with the same fire emissions but driven by different meteorological inputs, we have examined the sensitivity of modeled results to meteorological datasets. The discrepancy in modeled low visibility events arising from the use of different meteorological datasets is clearly evident, especially in the results of Bangkok and Kuching. However, using different meteorological input datasets does not appear to have influenced the modeled very low visibility events, or the severe haze events in the cities close to burning sites.

We have also examined the sensitivity of modeled results to the use of different emission inventories. We find that significant discrepancies of fire emissions in mainland Southeast Asia and northern Australia between the two emission inventories used in our study have caused a substantial difference in modeled fire aerosol concentration and visibility, especially in Bangkok and Singapore. For instance, the contribution to fire aerosol in Singapore from northern Australia changes from nearly zero in the simulation driven by FINNv1.5 to about 22% in another simulation driven by GFEDv4.1s. ~~We have also identified~~Based on these results, we suggest further research is needed to improve the ~~influence~~current estimate of the ~~difference in~~ spatiotemporal distribution ~~rather than~~of fire emissions, in addition to total emitted quantities from the fire hotspots ~~on modeled $PM_{2.5}$ concentration~~.

To further assess the impacts of particulate pollution on the surface visibility of the whole Southeast Asia and to estimate the fire aerosol's contribution, we have defined and derived a metric of "Haze Exposure Days" (HEDs), by integrating annual low visibility days of 50 cities of the Association of Southeast Asian Nations and weighted by population or averaged arithmetically. We find that a very large population of Southeast Asia has been exposed to relatively persistent hazy conditions. The top four cities in the HED ranking, Jakarta, Bangkok, Hanoi, and Yangon, with a total population exceeding ~~two millions~~30 million, all have experienced more than 200 days per year of low visibility due to particulate pollution over the past decade~~.~~ and more than 50% of those low visibility days were mainly due to fire aerosols. Even worse is that the number of annual low visibility days have been increasing steadily not only in high population cities but also those with relatively low populations, suggesting ~~a wide spread of~~widespread particulate ~~pollutions~~pollution across Southeast Asian. ~~Generally speaking~~In summary, the fire aerosols are found to be responsible for up to about half of the total ~~exposes~~exposures to low visibility in the region. ~~Our~~This result suggests that in order to improve the air quality in Southeast Asia, besides reducing or even prohibiting planned or unplanned fires, mitigation policies targeting ~~at~~ pollution sources other than fires ~~need~~also needs to be implemented ~~as well~~.

Acknowledgements.

This research was supported by the National Research Foundation Singapore through the Singapore-MIT Alliance for Research and Technology, the interdisciplinary research program of Center for Environmental Sensing and Modeling. It was also supported by

the U.S. National Science Foundation (AGS-1339264), U.S. DOE (DE-FG02-94ER61937) and U.S. EPA (XA-83600001-1). The authors would like to acknowledge the National Environment Agency (NEA) of Singapore for making Singapore $PM_{2.5}$ data available; the NCEP-FNL, ECMWF ERA-Interim, NCAR FINN, and GFED working groups for releasing their data to the research communities; and the NCAR WRF developing team for providing the numerical model for this study. We thank the National Supercomputing Centre of Singapore (NSCC) for providing computing resources and technical support. Two anonymous reviewers provided many constructive suggestions and comments, leading to a substantial improvement of the manuscript.

Reference

Carlson, K. M., Curran, L. M., Ratnasari, D., Pittman, A. M., Soares-Filho, B. S., Asner, G. P., Trigg, S. N., Gaveau, D. A., Lawrence, D., and Rodrigues, H. O.: Committed carbon emissions, deforestation, and community land conversion from oil palm plantation expansion in West Kalimantan, Indonesia, Proceedings of the National Academy of Sciences, 109, 7559-7564, 10.1073/pnas.1200452109, 2012.

Chang, C. P., Wang, Z., McBride, J., and Liu, C. H.: Annual Cycle of Southeast Asia—Maritime Continent Rainfall and the Asymmetric Monsoon Transition, Journal of Climate, 18, 287-301, 10.1175/JCLI-3257.1, 2005.

Dennis, R., Mayer, J., Applegate, G., Chokkalingam, U., Colfer, C. P., Kurniawan, I., Lachowski, H., Maus, P., Permana, R., Ruchiat, Y., Stolle, F., Suyanto, and Tomich, T.: Fire, People and Pixels: Linking Social Science and Remote Sensing to Understand Underlying Causes and Impacts of Fires in Indonesia, Hum Ecol, 33, 465-504, 10.1007/s10745-005-5156-z, 2005.

Emmanuel, S. C.: Impact to lung health of haze from forest fires: The Singapore experience, Respirology, 5, 175-182, 10.1046/j.1440-1843.2000.00247.x, 2000.

Field, R. D., van der Werf, G. R., and Shen, S. S. P.: Human amplification of drought-induced biomass burning in Indonesia since 1960, Nature Geosci, 2, 185-188, http://www.nature.com/ngeo/journal/v2/n3/suppinfo/ngeo443_S1.html, 2009.

Fujii, Y., Iriana, W., Oda, M., Puriwigati, A., Tohno, S., Lestari, P., Mizohata, A., and Huboyo, H. S.: Characteristics of carbonaceous aerosols emitted from peatland fire in Riau, Sumatra, Indonesia, Atmospheric Environment, 87, 164-169, http://dx.doi.org/10.1016/j.atmosenv.2014.01.037, 2014.

Giglio, L., Randerson, J. T., and van der Werf, G. R.: Analysis of daily, monthly, and annual burned area using the fourth-generation global fire emissions database (GFED4), Journal of Geophysical Research: Biogeosciences, 118, 317-328, 10.1002/jgrg.20042, 2013.

Grell, G., Freitas, S. R., Stuefer, M., and Fast, J.: Inclusion of biomass burning in WRF-Chem: impact of wildfires on weather forecasts, Atmos. Chem. Phys., 11, 5289-5303, 10.5194/acp-11-5289-2011, 2011.

Grell, G. A., Peckham, S. E., Schmitz, R., McKeen, S. A., Frost, G., Skamarock, W. C., and Eder, B.: Fully coupled "online" chemistry within the WRF model, Atmospheric Environment, 39, 10.1016/j.atmosenv.2005.04.027, 2005.

Heil, A., Langmann, B., and Aldrian, E.: Indonesian peat and vegetation fire emissions: Study on factors influencing large-scale smoke haze pollution using a regional atmospheric chemistry model, Mitig Adapt Strat Glob Change, 12, 113-133, 10.1007/s11027-006-9045-6, 2007.

Huffman, G. J., Bolvin, D. T., Nelkin, E. J., Wolff, D. B., Adler, R. F., Gu, G., Hong, Y., Bowman, K. P., and Stocker, E. F.: The TRMM Multisatellite Precipitation Analysis (TMPA): Quasi-Global, Multiyear, Combined-Sensor Precipitation Estimates at Fine Scales, Journal of Hydrometeorology, 8, 38-55, 10.1175/JHM560.1, 2007.

Johnston, F. H., Henderson, S. B., Chen, Y., Randerson, J. T., Marlier, M., Defries, R. S., Kinney, P., Bowman, D. M., and Brauer, M.: Estimated global mortality attributable to smoke from landscape fires Environ. Health Perspect. , 120 695-701, 2012.

Kiehl, J. T., Schneider, T. L., Rasch, P. J., Barth, M. C., and Wong, J.: Radiative forcing due to sulfate aerosols from simulations with the National Center for Atmospheric Research Community Climate Model, Version 3, Journal of Geophysical Research: Atmospheres, 105, 1441-1457, 10.1029/1999JD900495, 2000.

Kim, D., Wang, C., Ekman, A. M. L., Barth, M. C., and Rasch, P. J.: Distribution and direct radiative forcing of carbonaceous and sulfate aerosols in an interactive size-resolving aerosol–climate model, Journal of Geophysical Research: Atmospheres, 113, D16309, 10.1029/2007jd009756, 2008.

Koe, L. C. C., Arellano Jr, A. F., and McGregor, J. L.: Investigating the haze transport from 1997 biomass burning in Southeast Asia: its impact upon Singapore, Atmospheric Environment, 35, 2723-2734, http://dx.doi.org/10.1016/S1352-2310(00)00395-2, 2001.

Kunii, O., Kanagawa, S., Yajima, I., Hisamatsu, Y., Yamamura, S., Amagai, T., and Ismail, I. T. S.: The 1997 Haze Disaster in Indonesia: Its Air Quality and Health Effects, Archives of Environmental Health: An International Journal, 57, 16-22, 10.1080/00039890209602912, 2002.

Langner, A., Miettinen, J., and Siegert, F.: Land cover change 2002–2005 in Borneo and the role of fire derived from MODIS imagery, Global Change Biology, 13, 2329-2340, 10.1111/j.1365-2486.2007.01442.x, 2007.

Lin, N. H., Tsay, S. C., Maring, H. B., Yen, M. C., Sheu, G. R., Wang, S. H., Chi, K. H., Chuang, M. T., Ou-Yang, C. F., Fu, J. S., Reid, J. S., Lee, C. T., Wang, L. C., Wang, J. L., Hsu, C. N., Sayer, A. M., Holben, B. N., Chu, Y. C., Nguyen, X. A., Sopajaree, K., Chen, S. J., Cheng, M. T., Tsuang, B. J., Tsai, C. J., Peng, C. M.,

Schnell, R. C., Conway, T., Chang, C. T., Lin, K. S., Tsai, Y. I., Lee, W. J., Chang, S. C., Liu, J. J., Chiang, W. L., Huang, S. J., Lin, T. H., and Liu, G. R.: An overview of regional experiments on biomass burning aerosols and related pollutants in Southeast Asia: From BASE-ASIA and the Dongsha Experiment to 7-SEAS, Atmospheric Environment, 78, 1-19, http://dx.doi.org/10.1016/j.atmosenv.2013.04.066, 2013.

Madden, R. A., and Julian, P. R.: Detection of a 40–50 Day Oscillation in the Zonal Wind in the Tropical Pacific, Journal of the Atmospheric Sciences, 28, 702-708, 10.1175/1520-0469(1971)028<0702:DOADOI>2.0.CO;2, 1971.

Marlier, M., Defries, R. S., Kim, P. S., Koplitz, S. N., Jacob, D. J., Mickley, L. J., and Myers, S. S.: Fire emissions and regional air quality impacts from fires in oil palm, timber, and logging concessions in Indonesia, Environmental Research Letters, 10, 085005, 2015a.

Marlier, M. E., DeFries, R. S., Kim, P. S., Gaveau, D. L. A., Koplitz, S. N., Jacob, D. J., Mickley, L. J., Margono, B. A., and Myers, S. S.: Regional air quality impacts of future fire emissions in Sumatra and Kalimantan, Environmental Research Letters, 5, 054010 pp., 2015b.

Mauderly, J. L., and Chow, J. C.: Health effects of organic aerosols, Inhalation Toxicology, 20, 257-288, 2008.

McBride, J. L., Haylock, M. R., and Nicholls, N.: Relationships between the Maritime Continent Heat Source and the El Niño–Southern Oscillation Phenomenon, Journal of Climate, 16, 2905-2914, 10.1175/1520-0442(2003)016<2905:RBTMCH>2.0.CO;2, 2003.

Page, S. E., Siegert, F., Rieley, J. O., Boehm, H. D. V., Jaya, A., and Limin, S.: The amount of carbon released from peat and forest fires in Indonesia during 1997, Nature, 420, 61-65, 2002.

Randerson, J. T., Chen, Y., van der Werf, G. R., Rogers, B. M., and Morton, D. C.: Global burned area and biomass burning emissions from small fires, Journal of Geophysical Research: Biogeosciences, 117, G04012, 10.1029/2012JG002128, 2012.

Rasmusson, E. M., and Wallace, J. M.: Meteorological Aspects of the El Niño/Southern Oscillation, Science, 222, 1195-1202, 10.1126/science.222.4629.1195, 1983.

Reddington, C. L., Yoshioka, M., Balasubramanian, R., Ridley, D., Toh, Y. Y., Arnold, S. R., and Spracklen, D. V.: Contribution of vegetation and peat fires to particulate air pollution in Southeast Asia, Environmental Research Letters, 9, 094006, 2014.

Reid, J. S., Xian, P., Hyer, E. J., Flatau, M. K., Ramirez, E. M., Turk, F. J., Sampson, C. R., Zhang, C., Fukada, E. M., and Maloney, E. D.: Multi-scale meteorological conceptual analysis of observed active fire hotspot activity and smoke optical depth in the Maritime Continent, Atmos. Chem. Phys., 12, 2117-2147, 10.5194/acp-12-2117-2012, 2012.

Reid, J. S., Lagrosas, N. D., Jonsson, H. H., Reid, E. A., Sessions, W. R., Simpas, J. B., Uy, S. N., Boyd, T. J., Atwood, S. A., Blake, D. R., Campbell, J. R., Cliff, S. S., Holben, B. N., Holz, R. E., Hyer, E. J., Lynch, P., Meinardi, S., Posselt, D. J., Richardson, K. A., Salinas, S. V., Smirnov, A., Wang, Q., Yu, L., and Zhang, J.: Observations of the temporal variability in aerosol properties and their

relationships to meteorology in the summer monsoonal South China Sea/East Sea: the scale-dependent role of monsoonal flows, the Madden–Julian Oscillation, tropical cyclones, squall lines and cold pools, Atmos. Chem. Phys., 15, 1745-1768, 10.5194/acp-15-1745-2015, 2015.

Saji, N. H., Goswami, B. N., Vinayachandran, P. N., and Yamagata, T.: A dipole mode in the tropical Indian Ocean, Nature, 401, 360-363, 1999.

See, S. W., Balasubramanian, R., and Wang, W.: A study of the physical, chemical, and optical properties of ambient aerosol particles in Southeast Asia during hazy and nonhazy days, Journal of Geophysical Research: Atmospheres, 111, D10S08, 10.1029/2005JD006180, 2006.

Seinfeld, J., and Pandis, S.: Atmospheric Physics and Chemistry. From Air Pollution to Climate Change, Second Edition ed., New York (NY): JohnWiley & Sons, 2006.

Sekiguchi, M., Nakajima, T., Suzuki, K., Kawamoto, K., Higurashi, A., Rosenfeld, D., Sano, I., and Mukai, S.: A study of the direct and indirect effects of aerosols using global satellite data sets of aerosol and cloud parameters, Journal of Geophysical Research: Atmospheres, 108, 4699, 10.1029/2002JD003359, 2003.

Smith, A., Lott, N., and Vose, R.: The Integrated Surface Database: Recent Developments and Partnerships, Bulletin of the American Meteorological Society, 92, 704-708, doi:10.1175/2011BAMS3015.1, 2011.

Stauffer, D. R., and Seaman, N. L.: Multiscale Four-Dimensional Data Assimilation, Journal of Applied Meteorology, 33, 416-434, 10.1175/1520-0450(1994)033<0416:mfdda>2.0.co;2, 1994.

Tosca, M. G., Randerson, J. T., Zender, C. S., Nelson, D. L., Diner, D. J., and Logan, J. A.: Dynamics of fire plumes and smoke clouds associated with peat and deforestation fires in Indonesia, Journal of Geophysical Research: Atmospheres, 116, n/a-n/a, 10.1029/2010JD015148, 2011.

van der Werf, G. R., Randerson, J. T., Giglio, L., Collatz, G. J., Mu, M., Kasibhatla, P. S., Morton, D. C., DeFries, R. S., Jin, Y., and van Leeuwen, T. T.: Global fire emissions and the contribution of deforestation, savanna, forest, agricultural, and peat fires (1997–2009), Atmos. Chem. Phys., 10, 11707-11735, 10.5194/acp-10-11707-2010, 2010.

Visscher, A. D.: Air Dispersion Modeling: Foundations and Applications, First ed., John Wiley & Sons, Inc., 2013.

Wang, J., Ge, C., Yang, Z., Hyer, E. J., Reid, J. S., Chew, B. N., Mahmud, M., Zhang, Y., and Zhang, M.: Mesoscale modeling of smoke transport over the Southeast Asian Maritime Continent: Interplay of sea breeze, trade wind, typhoon, and topography, Atmospheric Research, 122, 486-503, http://dx.doi.org/10.1016/j.atmosres.2012.05.009, 2013.

Wiedinmyer, C., Akagi, S. K., Yokelson, R. J., Emmons, L. K., Al-Saadi, J. A., Orlando, J. J., and Soja, A. J.: The Fire INventory from NCAR (FINN): a high resolution global model to estimate the emissions from open burning, Geosci. Model Dev., 4, 625-641, 10.5194/gmd-4-625-2011, 2011.

Wu, C. H., and Hsu, H. H.: Topographic Influence on the MJO in the Maritime Continent, Journal of Climate, 22, 5433-5448, 10.1175/2009JCLI2825.1, 2009.

Wu, R., Wen, Z., and He, Z.: ENSO Contribution to Aerosol Variations over the Maritime Continent and the Western North Pacific during 2000–10, Journal of Climate, 26, 6541-6560, 10.1175/JCLI-D-12-00253.1, 2013.
Zhang, C.: Madden-Julian Oscillation, Reviews of Geophysics, 43, RG2003, 10.1029/2004RG000158, 2005.
Carlson, K. M., Curran, L. M., Ratnasari, D., Pittman, A. M., Soares-Filho, B. S., Asner, G. P., Trigg, S. N., Gaveau, D. A., Lawrence, D., and Rodrigues, H. O.: Committed carbon emissions, deforestation, and community land conversion from oil palm plantation expansion in West Kalimantan, Indonesia, Proceedings of the National Academy of Sciences, 109, 7559-7564, 10.1073/pnas.1200452109, 2012.
Chang, C. P., Wang, Z., McBride, J., and Liu, C.-H.: Annual Cycle of Southeast Asia—Maritime Continent Rainfall and the Asymmetric Monsoon Transition, Journal of Climate, 18, 287-301, 10.1175/JCLI-3257.1, 2005.
Crippa, P., Castruccio, S., Archer-Nicholls, S., Lebron, G. B., Kuwata, M., Thota, A., Sumin, S., Butt, E., Wiedinmyer, C., and Spracklen, D. V.: Population exposure to hazardous air quality due to the 2015 fires in Equatorial Asia, Scientific Reports, 6, 37074, 10.1038/srep37074, 2016.
Dennis, R., Mayer, J., Applegate, G., Chokkalingam, U., Colfer, C. P., Kurniawan, I., Lachowski, H., Maus, P., Permana, R., Ruchiat, Y., Stolle, F., Suyanto, and Tomich, T.: Fire, People and Pixels: Linking Social Science and Remote Sensing to Understand Underlying Causes and Impacts of Fires in Indonesia, Hum Ecol, 33, 465-504, 10.1007/s10745-005-5156-z, 2005.
Emmanuel, S. C.: Impact to lung health of haze from forest fires: The Singapore experience, Respirology, 5, 175-182, 10.1046/j.1440-1843.2000.00247.x, 2000.
European Centre for Medium-Range Weather, F.: ERA-Interim Project, 10.5065/D6CR5RD9, 2009.
Field, R. D., van der Werf, G. R., and Shen, S. S. P.: Human amplification of drought-induced biomass burning in Indonesia since 1960, Nature Geosci, 2, 185-188, http://www.nature.com/ngeo/journal/v2/n3/suppinfo/ngeo443_S1.html, 2009.
Fujii, Y., Iriana, W., Oda, M., Puriwigati, A., Tohno, S., Lestari, P., Mizohata, A., and Huboyo, H. S.: Characteristics of carbonaceous aerosols emitted from peatland fire in Riau, Sumatra, Indonesia, Atmospheric Environment, 87, 164-169, http://dx.doi.org/10.1016/j.atmosenv.2014.01.037, 2014.
Giglio, L., Randerson, J. T., and van der Werf, G. R.: Analysis of daily, monthly, and annual burned area using the fourth-generation global fire emissions database (GFED4), Journal of Geophysical Research: Biogeosciences, 118, 317-328, 10.1002/jgrg.20042, 2013.
Grandey, B. S., Lee, H. H., and Wang, C.: Radiative effects of interannually varying vs. interannually invariant aerosol emissions from fires, Atmos. Chem. Phys., 16, 14495-14513, 10.5194/acp-16-14495-2016, 2016.
Grell, G., Freitas, S. R., Stuefer, M., and Fast, J.: Inclusion of biomass burning in WRF-Chem: impact of wildfires on weather forecasts, Atmos. Chem. Phys., 11, 5289-5303, 10.5194/acp-11-5289-2011, 2011.

908 Grell, G. A., Peckham, S. E., Schmitz, R., McKeen, S. A., Frost, G., Skamarock, W. C., and
909 Eder, B.: Fully coupled "online" chemistry within the WRF model,
910 Atmospheric Environment, 39, 10.1016/j.atmosenv.2005.04.027, 2005.
911 Heil, A., Langmann, B., and Aldrian, E.: Indonesian peat and vegetation fire
912 emissions: Study on factors influencing large-scale smoke haze pollution
913 using a regional atmospheric chemistry model, Mitig Adapt Strat Glob
914 Change, 12, 113-133, 10.1007/s11027-006-9045-6, 2007.
915 Huffman, G. J., Bolvin, D. T., Nelkin, E. J., Wolff, D. B., Adler, R. F., Gu, G., Hong, Y.,
916 Bowman, K. P., and Stocker, E. F.: The TRMM Multisatellite Precipitation
917 Analysis (TMPA): Quasi-Global, Multiyear, Combined-Sensor Precipitation
918 Estimates at Fine Scales, Journal of Hydrometeorology, 8, 38-55,
919 10.1175/JHM560.1, 2007.
920 IEA: Energy and Climate Change, World Energy Outlook Special Report,
921 International Energy Agency, pp. 74 -77, 2015.
922 Johnston, F. H., Henderson, S. B., Chen, Y., Randerson, J. T., Marlier, M., Defries, R. S.,
923 Kinney, P., Bowman, D. M., and Brauer, M.: Estimated global mortality
924 attributable to smoke from landscape fires Environ. Health Perspect. , 120
925 695–701, 2012.
926 Kiehl, J. T., Schneider, T. L., Rasch, P. J., Barth, M. C., and Wong, J.: Radiative forcing
927 due to sulfate aerosols from simulations with the National Center for
928 Atmospheric Research Community Climate Model, Version 3, Journal of
929 Geophysical Research: Atmospheres, 105, 1441-1457,
930 10.1029/1999JD900495, 2000.
931 Kim, D., Wang, C., Ekman, A. M. L., Barth, M. C., and Rasch, P. J.: Distribution and
932 direct radiative forcing of carbonaceous and sulfate aerosols in an interactive
933 size-resolving aerosol–climate model, Journal of Geophysical Research:
934 Atmospheres, 113, D16309, 10.1029/2007jd009756, 2008.
935 Koe, L. C. C., Arellano Jr, A. F., and McGregor, J. L.: Investigating the haze transport
936 from 1997 biomass burning in Southeast Asia: its impact upon Singapore,
937 Atmospheric Environment, 35, 2723-2734,
938 http://dx.doi.org/10.1016/S1352-2310(00)00395-2, 2001.
939 Kunii, O., Kanagawa, S., Yajima, I., Hisamatsu, Y., Yamamura, S., Amagai, T., and
940 Ismail, I. T. S.: The 1997 Haze Disaster in Indonesia: Its Air Quality and Health
941 Effects, Archives of Environmental Health: An International Journal, 57, 16-
942 22, 10.1080/00039890209602912, 2002.
943 Langner, A., Miettinen, J., and Siegert, F.: Land cover change 2002–2005 in Borneo
944 and the role of fire derived from MODIS imagery, Global Change Biology, 13,
945 2329-2340, 10.1111/j.1365-2486.2007.01442.x, 2007.
946 Lin, N.-H., Tsay, S.-C., Maring, H. B., Yen, M.-C., Sheu, G.-R., Wang, S.-H., Chi, K. H.,
947 Chuang, M.-T., Ou-Yang, C.-F., Fu, J. S., Reid, J. S., Lee, C.-T., Wang, L.-C., Wang,
948 J.-L., Hsu, C. N., Sayer, A. M., Holben, B. N., Chu, Y.-C., Nguyen, X. A., Sopajaree,
949 K., Chen, S.-J., Cheng, M.-T., Tsuang, B.-J., Tsai, C.-J., Peng, C.-M., Schnell, R. C.,
950 Conway, T., Chang, C.-T., Lin, K.-S., Tsai, Y. I., Lee, W.-J., Chang, S.-C., Liu, J.-J.,
951 Chiang, W.-L., Huang, S.-J., Lin, T.-H., and Liu, G.-R.: An overview of regional
952 experiments on biomass burning aerosols and related pollutants in Southeast
953 Asia: From BASE-ASIA and the Dongsha Experiment to 7-SEAS, Atmospheric

954 Environment, 78, 1-19, http://dx.doi.org/10.1016/j.atmosenv.2013.04.066,
955 2013.
956 Madden, R. A., and Julian, P. R.: Detection of a 40–50 Day Oscillation in the Zonal
957 Wind in the Tropical Pacific, Journal of the Atmospheric Sciences, 28, 702-
958 708, 10.1175/1520-0469(1971)028<0702:DOADOI>2.0.CO;2, 1971.
959 Marlier, M., Defries, R. S., Kim, P. S., Koplitz, S. N., Jacob, D. J., Mickley, L. J., and Myers,
960 S. S.: Fire emissions and regional air quality impacts from fires in oil palm,
961 timber, and logging concessions in Indonesia, Environmental Research
962 Letters, 10, 085005, 2015a.
963 Marlier, M. E., DeFries, R. S., Kim, P. S., Gaveau, D. L. A., Koplitz, S. N., Jacob, D. J.,
964 Mickley, L. J., Margono, B. A., and Myers, S. S.: Regional air quality impacts of
965 future fire emissions in Sumatra and Kalimantan, Environmental Research
966 Letters, 5, 054010 pp., 2015b.
967 Mauderly, J. L., and Chow, J. C.: Health effects of organic aerosols, Inhalation
968 Toxicology, 20, 257-288, 2008.
969 McBride, J. L., Haylock, M. R., and Nicholls, N.: Relationships between the Maritime
970 Continent Heat Source and the El Niño–Southern Oscillation Phenomenon,
971 Journal of Climate, 16, 2905-2914, 10.1175/1520-
972 0442(2003)016<2905:RBTMCH>2.0.CO;2, 2003.
973 Page, S. E., Siegert, F., Rieley, J. O., Boehm, H.-D. V., Jaya, A., and Limin, S.: The amount
974 of carbon released from peat and forest fires in Indonesia during 1997,
975 Nature, 420, 61-65, 2002.
976 Randerson, J. T., Chen, Y., van der Werf, G. R., Rogers, B. M., and Morton, D. C.: Global
977 burned area and biomass burning emissions from small fires, Journal of
978 Geophysical Research: Biogeosciences, 117, G04012,
979 10.1029/2012JG002128, 2012.
980 Rasmusson, E. M., and Wallace, J. M.: Meteorological Aspects of the El Niño/Southern
981 Oscillation, Science, 222, 1195-1202, 10.1126/science.222.4629.1195, 1983.
982 Reddington, C. L., Yoshioka, M., Balasubramanian, R., Ridley, D., Toh, Y. Y., Arnold, S.
983 R., and Spracklen, D. V.: Contribution of vegetation and peat fires to
984 particulate air pollution in Southeast Asia, Environmental Research Letters,
985 9, 094006, 2014.
986 Reid, J. S., Xian, P., Hyer, E. J., Flatau, M. K., Ramirez, E. M., Turk, F. J., Sampson, C. R.,
987 Zhang, C., Fukada, E. M., and Maloney, E. D.: Multi-scale meteorological
988 conceptual analysis of observed active fire hotspot activity and smoke optical
989 depth in the Maritime Continent, Atmos. Chem. Phys., 12, 2117-2147,
990 10.5194/acp-12-2117-2012, 2012.
991 Reid, J. S., Lagrosas, N. D., Jonsson, H. H., Reid, E. A., Sessions, W. R., Simpas, J. B., Uy,
992 S. N., Boyd, T. J., Atwood, S. A., Blake, D. R., Campbell, J. R., Cliff, S. S., Holben, B.
993 N., Holz, R. E., Hyer, E. J., Lynch, P., Meinardi, S., Posselt, D. J., Richardson, K. A.,
994 Salinas, S. V., Smirnov, A., Wang, Q., Yu, L., and Zhang, J.: Observations of the
995 temporal variability in aerosol properties and their relationships to
996 meteorology in the summer monsoonal South China Sea/East Sea: the scale-
997 dependent role of monsoonal flows, the Madden–Julian Oscillation, tropical
998 cyclones, squall lines and cold pools, Atmos. Chem. Phys., 15, 1745-1768,
999 10.5194/acp-15-1745-2015, 2015.

Saji, N. H., Goswami, B. N., Vinayachandran, P. N., and Yamagata, T.: A dipole mode in the tropical Indian Ocean, Nature, 401, 360-363, 1999.

See, S. W., Balasubramanian, R., and Wang, W.: A study of the physical, chemical, and optical properties of ambient aerosol particles in Southeast Asia during hazy and nonhazy days, Journal of Geophysical Research: Atmospheres, 111, D10S08, 10.1029/2005JD006180, 2006.

Seinfeld, J., and Pandis, S.: Atmospheric Physics and Chemistry. From Air Pollution to Climate Change, Second Edition ed., New York (NY): JohnWiley & Sons, 2006.

Sekiguchi, M., Nakajima, T., Suzuki, K., Kawamoto, K., Higurashi, A., Rosenfeld, D., Sano, I., and Mukai, S.: A study of the direct and indirect effects of aerosols using global satellite data sets of aerosol and cloud parameters, Journal of Geophysical Research: Atmospheres, 108, 4699, 10.1029/2002JD003359, 2003.

Smith, A., Lott, N., and Vose, R.: The Integrated Surface Database: Recent Developments and Partnerships, Bulletin of the American Meteorological Society, 92, 704-708, doi:10.1175/2011BAMS3015.1, 2011.

Stauffer, D. R., and Seaman, N. L.: Multiscale Four-Dimensional Data Assimilation, Journal of Applied Meteorology, 33, 416-434, 10.1175/1520-0450(1994)033<0416:mfdda>2.0.co;2, 1994.

Tosca, M. G., Randerson, J. T., Zender, C. S., Nelson, D. L., Diner, D. J., and Logan, J. A.: Dynamics of fire plumes and smoke clouds associated with peat and deforestation fires in Indonesia, Journal of Geophysical Research: Atmospheres, 116, n/a-n/a, 10.1029/2010JD015148, 2011.

van der Werf, G. R., Randerson, J. T., Giglio, L., Collatz, G. J., Mu, M., Kasibhatla, P. S., Morton, D. C., DeFries, R. S., Jin, Y., and van Leeuwen, T. T.: Global fire emissions and the contribution of deforestation, savanna, forest, agricultural, and peat fires (1997–2009), Atmos. Chem. Phys., 10, 11707-11735, 10.5194/acp-10-11707-2010, 2010.

Visscher, A. D.: Air Dispersion Modeling: Foundations and Applications, First ed., John Wiley & Sons, Inc., 2013.

Wang, J., Ge, C., Yang, Z., Hyer, E. J., Reid, J. S., Chew, B.-N., Mahmud, M., Zhang, Y., and Zhang, M.: Mesoscale modeling of smoke transport over the Southeast Asian Maritime Continent: Interplay of sea breeze, trade wind, typhoon, and topography, Atmospheric Research, 122, 486-503, http://dx.doi.org/10.1016/j.atmosres.2012.05.009, 2013.

Wiedinmyer, C., Akagi, S. K., Yokelson, R. J., Emmons, L. K., Al-Saadi, J. A., Orlando, J. J., and Soja, A. J.: The Fire INventory from NCAR (FINN): a high resolution global model to estimate the emissions from open burning, Geosci. Model Dev., 4, 625-641, 10.5194/gmd-4-625-2011, 2011.

Wu, C.-H., and Hsu, H.-H.: Topographic Influence on the MJO in the Maritime Continent, Journal of Climate, 22, 5433-5448, 10.1175/2009JCLI2825.1, 2009.

Wu, R., Wen, Z., and He, Z.: ENSO Contribution to Aerosol Variations over the Maritime Continent and the Western North Pacific during 2000–10, Journal of Climate, 26, 6541-6560, 10.1175/JCLI-D-12-00253.1, 2013.

Zhang, C.: Madden-Julian Oscillation, Reviews of Geophysics, 43, RG2003, 10.1029/2004RG000158, 2005.

Table 1. WRF physics scheme configuration

Physics Processes	Scheme
microphysics	Morrison (2 moments) scheme
longwave radiation	rrtmg scheme
shortwave radiation	rrtmg scheme
surface-layer	MYNN surface layer
land surface	Unified Noah land-surface model
planetary boundary layer	MYNN 2.5 level TKE scheme
cumulus parameterization	Grell-Freitas ensemble scheme

	~~FNL_FINN vs. TRMM~~		~~ERA_FINN vs. TRMM~~	
	~~Spatial cor.~~	~~Temporal cor.~~	~~Spatial cor.~~	~~Temporal cor.~~
~~FMA~~	~~0.89~~	~~0.61~~	~~0.89~~	~~0.89~~
~~MJJ~~	~~0.83~~	~~0.69~~	~~0.81~~	~~0.90~~
~~ASO~~	~~0.86~~	~~0.59~~	~~0.84~~	~~0.89~~
~~NDJ~~	~~0.88~~	~~0.60~~	~~0.88~~	~~0.85~~
~~All~~	~~0.86~~	~~0.68~~	~~0.85~~	~~0.90~~

Table 2.
Annual mean low visibility days (LVDs; observed visibility ≤ 10 km) and very low visibility days (VLVDs; observed visibility ≤ 7 km) per year in Bangkok, Kuala Lumpur, Singapore and Kuching during 2003-2014 are presented in the second column. Parentheses show the percentage of year. The third ~~and fourth columns show the percentage contributions~~column shows the percentages, along with standard deviations, of ~~fire and~~ low visibility days explained by fire aerosols alone (i.e. the LVDs captured by the model). The fourth column is the same as the third column but for non-fire (other) pollutions ~~for total low visibility days.~~, which is calculated as 100% - fire pollution contribution (i.e. the percentage of LVDs not captured by the model).

FNL_FINN	**LVD per year (days)**	**Fire pollution contribution (%)**	**Other pollution contribution (%)**
Bangkok, Thailand	215±50 (59±14%)	39±8	61±8
Kuala Lumpur, Malaysia	174±78 (48±21%)	36±17	64±17
Singapore, Singapore	96±87 (26±24%)	34±17	66±17
Kuching, Malaysia	95±57 (26±17%)	33±15	67±15
FNL_FINN	**VLVD per year (days)**	**Fire pollution contribution (%)**	**Other pollution contribution (%)**
Bangkok, Thailand	15±8 (4±2%)	87±20	~~87~~13±20
Kuala Lumpur, Malaysia	19±18 (5±5%)	85±17	15±17
Singapore, Singapore	4±4 (1±1%)	91±33	9±33
Kuching, Malaysia	22±18 (6±5%)	93±11	7±11
ERA_FINN	**~~VLD~~LVD per year (days)**	**Fire pollution contribution (%)**	**Other pollution contribution (%)**
Bangkok, Thailand	215±50 (59±14%)	46±7	54±7
Kuala Lumpur, Malaysia	174±78 (48±21%)	40±16	60±16
Singapore, Singapore	96±87 (26±24%)	37±18	63±18
Kuching, Malaysia	95±57 (26±17%)	45±17	55±17
ERA_FINN	**VLVD per year (days)**	**Fire pollution contribution (%)**	**Other pollution contribution (%)**
Bangkok, Thailand	15±8 (4±2%)	88±20	12±20
Kuala Lumpur, Malaysia	19±18 (5±5%)	90±18	10±18
Singapore, Singapore	4±4 (1±1%)	98±6	2±6
Kuching, Malaysia	22±18 (6±5%)	94±11	6±11
FNL_GFED	**~~VLD~~LVD per year (days)**	**Fire pollution contribution (%)**	**Other pollution contribution (%)**
Bangkok, Thailand	215±50 (59±14%)	36±8	64±8
Kuala Lumpur, Malaysia	174±78 (48±21%)	28±17	72±17
Singapore, Singapore	96±87 (26±24%)	29±21	71±21
Kuching, Malaysia	95±57 (26±17%)	26±18	74±18
FNL_GFED	**VLVD per year (days)**	**Fire pollution contribution (%)**	**Other pollution contribution (%)**
Bangkok, Thailand	15±8 (4±2%)	90±19	10±19
Kuala Lumpur, Malaysia	19±18 (5±5%)	83±28	17±28
Singapore, Singapore	4±4 (1±1%)	89±37	11±37
Kuching, Malaysia	22±18 (6±5%)	89±28	11±28

1067

Table 43. Annual mean and standard deviation of modeled fire $PM_{2.5}$ concentration (μg m^{-3}) ~~contributed by each source region~~ in Bangkok, Kuala Lumpur, Singapore, and Kuching during 2003-2014~~.~~ contributed by each source region (s1 – s5). Parentheses show the percentage of fire $PM_{2.5}$ contribution originating from each source region. ~~The same regions,~~Regions s1-s5~~,~~ are ~~explained~~defined in Fig. 1. FNL_FINN, ERA_FINN and FNL_GFED are three model simulations descried in Section 2.1.

FNL_FINN	s1	s2	s3	s4	s5
Bangkok	8.4±2.3 (99.2±0.5%)	0.0±0.0 (0.1±0.1%)	0.0±0.0 (0.1±0.1%)	0.1±0.0 (0.6±0.5%)	0.0±0.0 (0.0±0.0%)
Kuala Lumpur	2.3±1.2 (43.3±14.8%)	2.7±1.4 (49.6±14.9%)	0.2±0.2 (3.3±3.4%)	0.1±0.1 (2.5±2.3%)	0.0±0.0 (0.3±0.2%)
Singapore	1.1±0.7 (36.7±14.7%)	1.2±0.8 (40.7±15.9%)	0.4±0.4 (14.3±10.0%)	0.2±0.1 (6.1±3.8%)	0.1±0.0 (2.2±1.1%)
Kuching	0.5±0.4 (7.8±6.5%)	0.3±0.1 (4.7±2.5%)	6.0±3.2 (84.6±9.7%)	0.1±0.1 (2.3±2.5%)	0.0±0.0 (0.6±0.3%)
ERA_FINN	s1	s2	s3	s4	s5
Bangkok	9.1±2.3 (99.2±0.4%)	0.0±0.0 (0.1±0.1%)	0.0±0.0 (0.1±0.1%)	0.1±0.0 (0.6±0.4%)	0.0±0.0 (0.0±0.0%)
Kuala Lumpur	2.3±1.2 (39.7±12.7%)	3.2±1.4 (53.7±12.3%)	0.2±0.2 (3.9±3.3%)	0.1±0.0 (2.3±1.8%)	0.0±0.0 (0.4±0.2%)
Singapore	1.1±0.6 (34.2±13.5%)	1.4±0.9 (40.5±13.7%)	0.6±0.6 (17.2±11.8%)	0.2±0.1 (6.2±3.1%)	0.1±0.0 (1.9±0.9%)
Kuching	0.5±0.4 (8.1±5.6%)	0.4±0.2 (6.1±3.9%)	6.7±3.9 (82.5±10.0%)	0.1±0.1 (2.7±3.0%)	0.0±0.0 (0.6±0.3%)
FNL_GFED	s1	s2	s3	s4	s5
Bangkok	4.8±1.3 (99.6±0.2%)	0.0±0.0 (0.1±0.0%)	0.0±0.0 (0.1±0.1%)	0.0±0.0 (0.2±0.2%)	0.0±0.0 (0.1±0.0%)
Kuala Lumpur	1.3±0.6 (38.6±20.8%)	2.7±1.9 (53.8±21.1%)	0.1±0.2 (2.8±3.5%)	0.0±0.0 (0.8±0.8%)	0.1±0.1 (3.9±3.4%)
Singapore	0.3±0.2 (22.1±17.3%)	1.5±1.8 (40.2±23.6%)	0.4±0.5 (12.5±9.5%)	0.1±0.0 (2.9±2.4%)	0.4±0.2 (22.3±13.2%)
Kuching	0.1±0.1 (7.2±6.8%)	0.1±0.1 (4.3±3.2%)	3.2±3.2 (75.2±12.9%)	0.0±0.0 (1.7±2.7%)	0.3±0.2 (11.6±6.7%)

Table 4. The spatial and temporal correlation of monthly rainfall between models (FNL_FINN and ERA_FINN) and observation (TRMM) during 2003-2014. FMA, MJJ, ASO, NDJ and All represents February-April, May-July, August-October, November-January and whole year, respectively.

	FNL_FINN vs. TRMM		ERA_FINN vs. TRMM	
	Spatial cor.	Temporal cor.	Spatial cor.	Temporal cor.
FMA	0.89	0.61	0.89	0.89
MJJ	0.83	0.69	0.81	0.90
ASO	0.86	0.59	0.84	0.89
NDJ	0.88	0.60	0.88	0.85
All	0.86	0.68	0.85	0.90

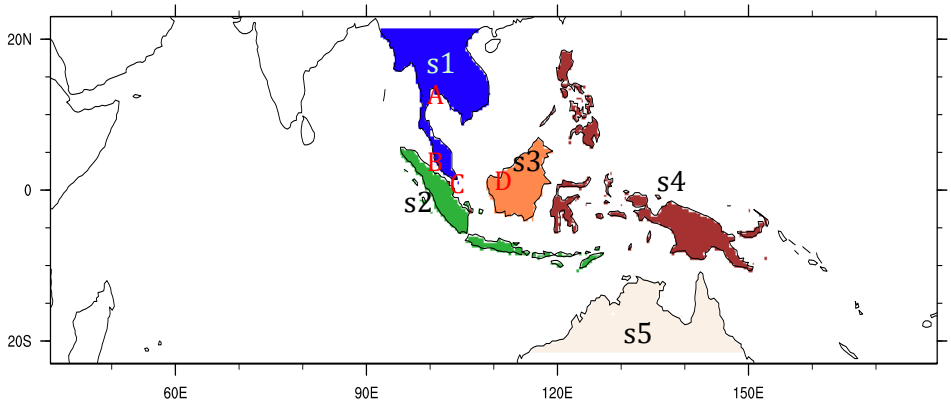

Figure 1. Model domain used for simulations. The domain has 432 × 148 grid points with a horizontal resolution of 36 km. Five fire source regions marked in different colors and labeled as s1, s2, s3, s4 and s5, represent mainland Southeast Asia (s1), Sumatra and Java islands (s2), Borneo (s3), the rest of Maritime Continent (s4), and northern Australia (s5). A, B, C and D indicate the location of four selected cities: Bangkok (A), Kuala Lumpur (B), Singapore (C) and Kuching (D).

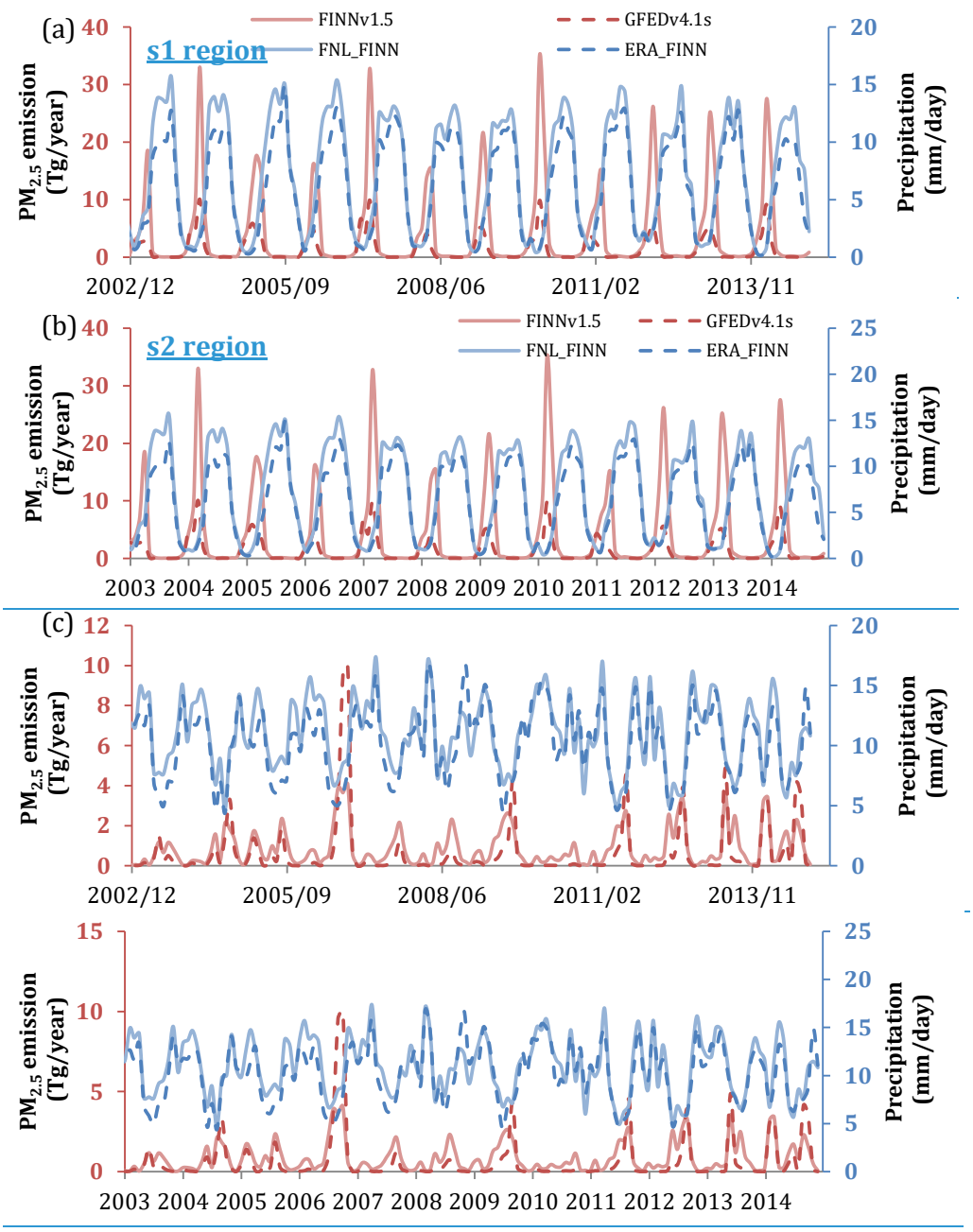
(a)
s1 region
FINNv1.5
FNL_FINN
GFEDv4.1s
ERA_FINN
PM2.5 emission (Tg/year)
Precipitation (mm/day)
2002/12
2005/09
2008/06
2011/02
2013/11
(b)
s2 region
2003 2004 2005 2006 2007 2008 2009 2010 2011 2012 2013 2014
(c)

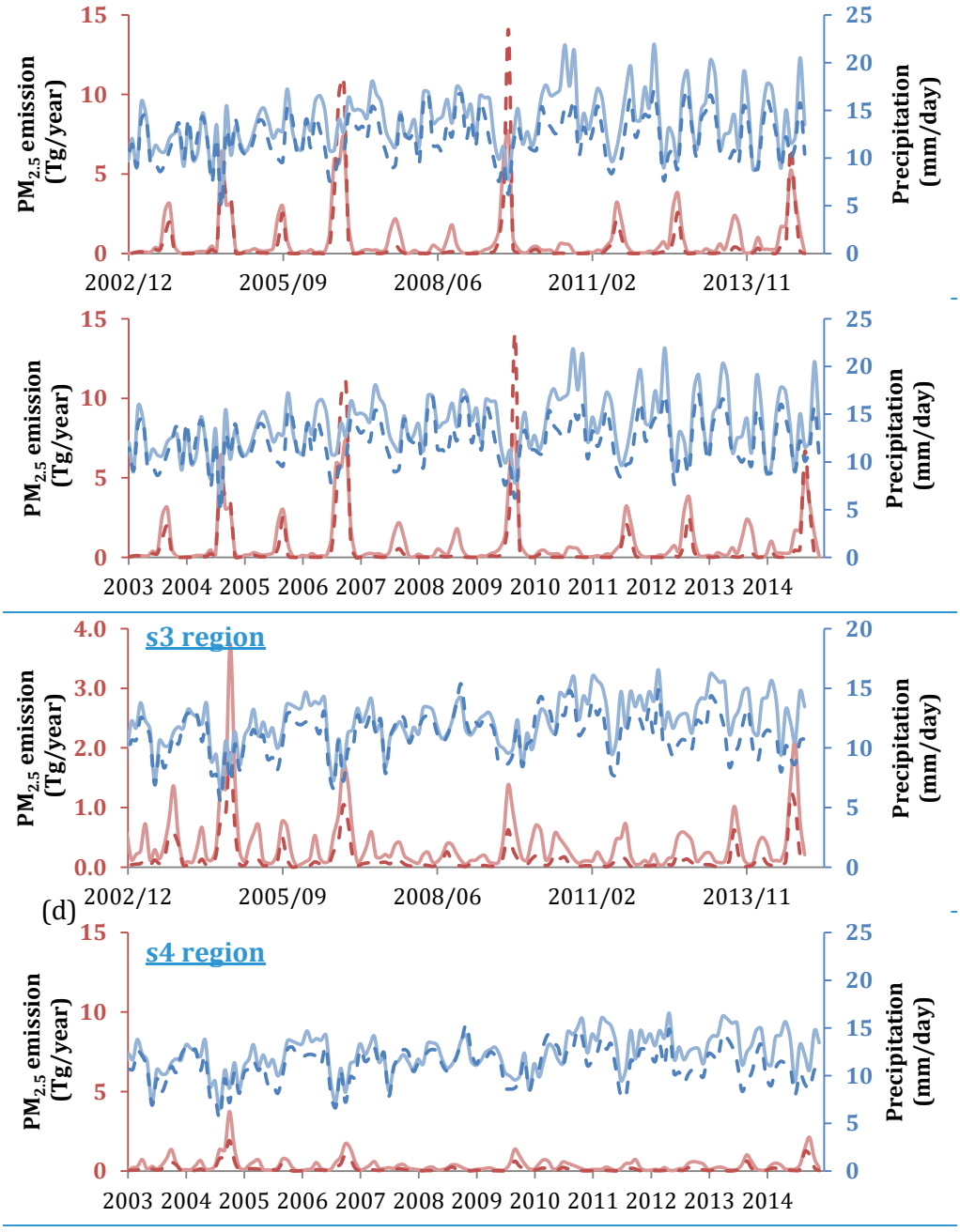
PM2.5 emission (Tg/year)
Precipitation (mm/day)
2002/12
2005/09
2008/06
2011/02
2013/11
2003 2004 2005 2006 2007 2008 2009 2010 2011 2012 2013 2014
s3 region
s4 region

(d)

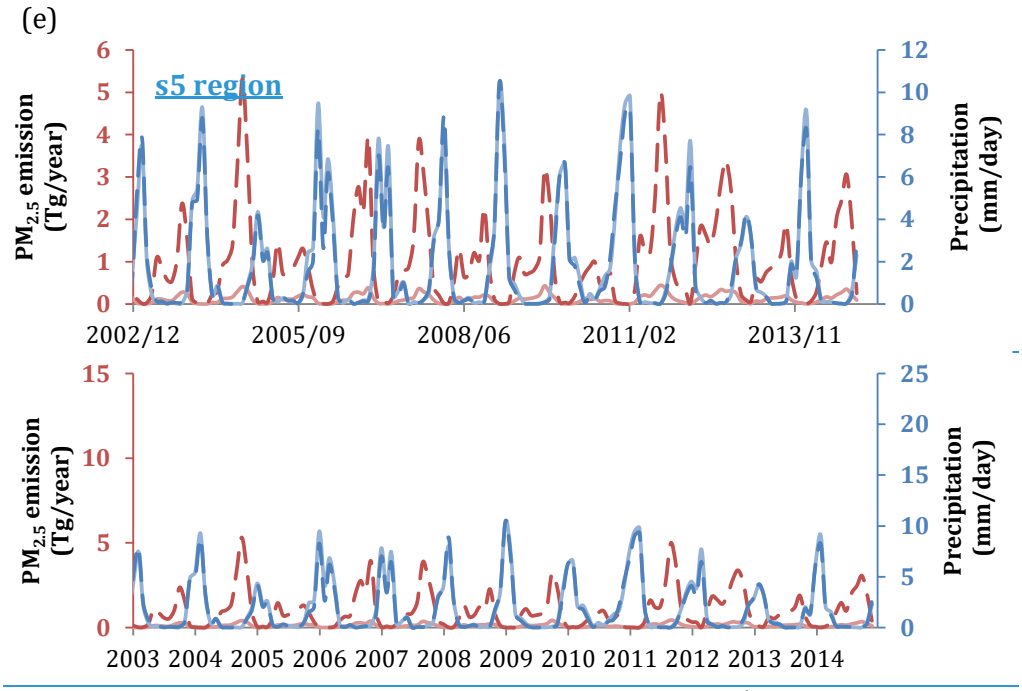

Figure 2. Time series of monthly $PM_{2.5}$ emission (Tg $year^{-1}$) in FINNv1.5 (pink solid lines) and GFEDv4.1s (red dashed lines). Also shown are precipitation rates (mm day^{-1}) simulated in FNL_FINN (light blue solid lines) and ERA_FINN (blue dashed lines) during 2003-2014 in: (a) mainland Southeast Asia (s1), (b) Sumatra and Java islands (s2), (c) Borneo (s3), (d) the rest of the Maritime Continent (s4), and (e) northern Australia (s5).

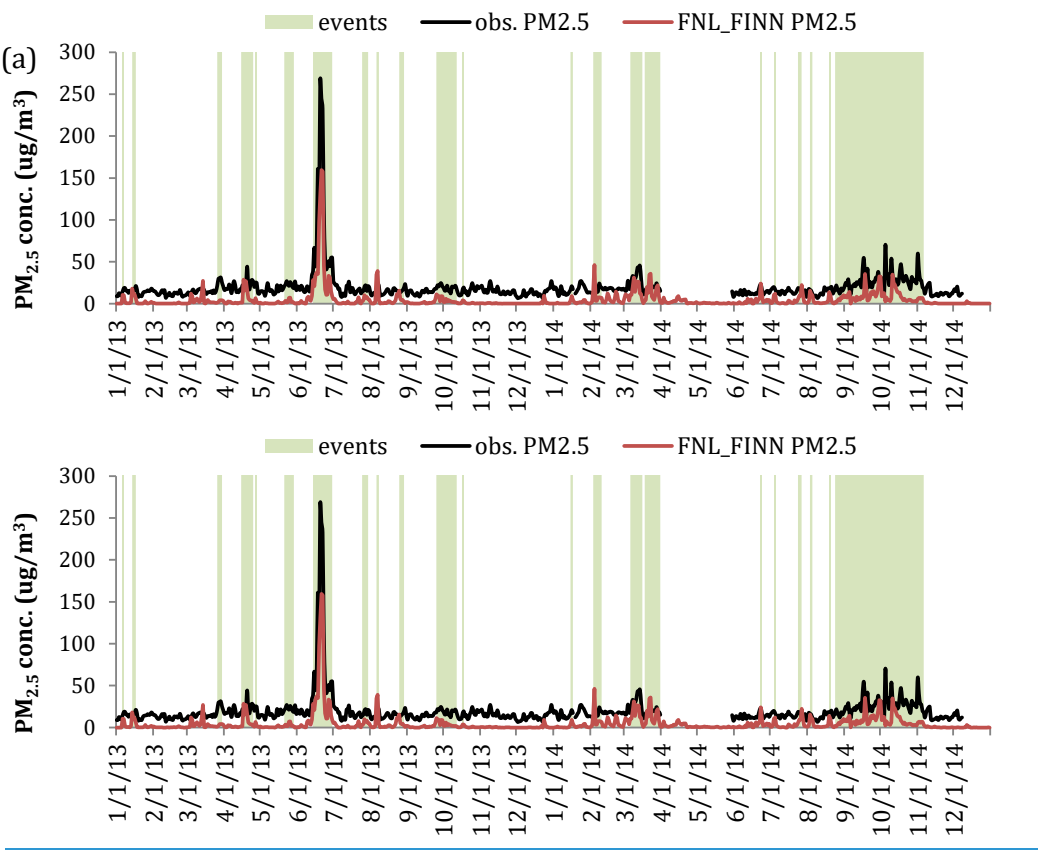
(a)
events
obs. PM2.5
FNL_FINN PM2.5
PM2.5 conc. (ug/m3)
300
250
200
150
100
50
0
1/1/13
2/1/13
3/1/13
4/1/13
5/1/13
6/1/13
7/1/13
8/1/13
9/1/13
10/1/13
11/1/13
12/1/13
1/1/14
2/1/14
3/1/14
4/1/14
5/1/14
6/1/14
7/1/14
8/1/14
9/1/14
10/1/14
11/1/14
12/1/14
events
obs. PM2.5
FNL_FINN PM2.5
PM2.5 conc. (ug/m3)

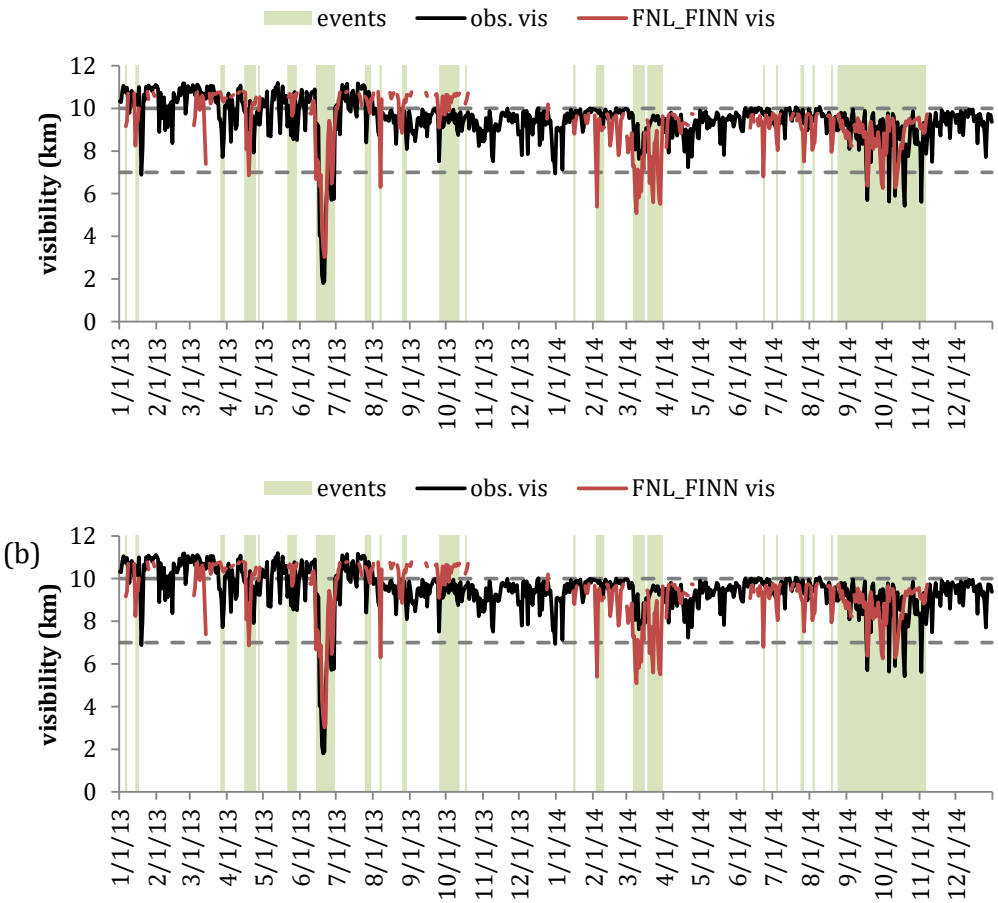

Figure 3. (a) Time series of daily surface $PM_{2.5}$ from the ground-based observations (black line) and FNL_FINN simulated results (red line) in Singapore during 2013-2014. (b) ~~Time series of~~Same as (a) but daily visibility ~~of~~from GSOD ~~observation~~observations (black line) and calculated result from FNL_FINN (red line~~) in Singapore during 2013-2014.~~). Highlighted green areas are known haze events caused by fire aerosols, which are reported by news or manually selected based on observed $PM_{2.5}$. Two gray lines mark the visibility of 7 and 10 km, respectively.

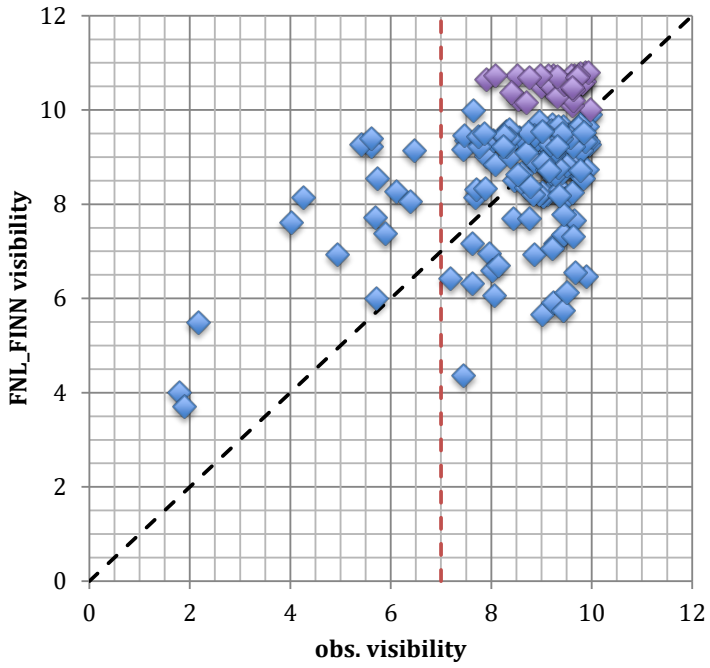

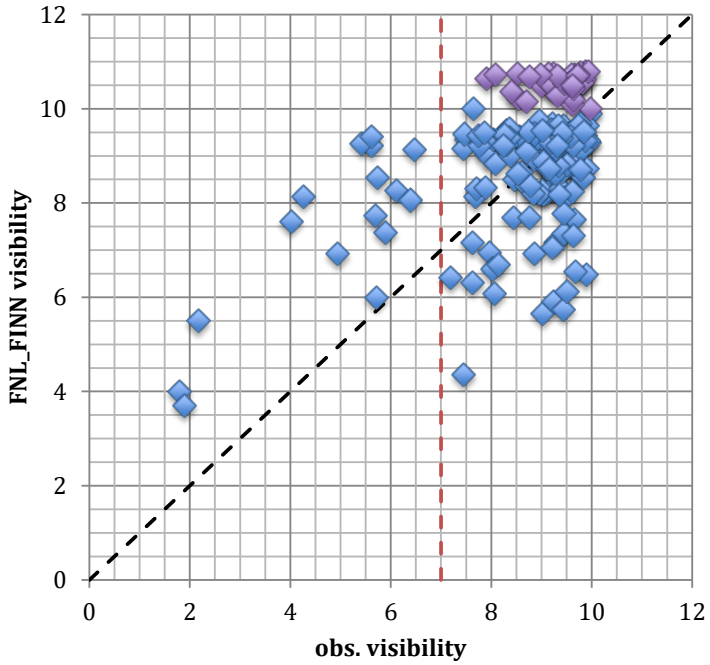

Figure 4. A scatter plot of observed visibility and FNL_FINN visibility during known fire events as labeled in Fig. ~~4b~~3b. Black dash line refers 1:1 line and red line is the threshold of VLVD (7 km). ~~Data~~Purple points ~~marked with purple color are~~remark the known low visibility events that model failed to produce a visibility at least qualified for LVD.

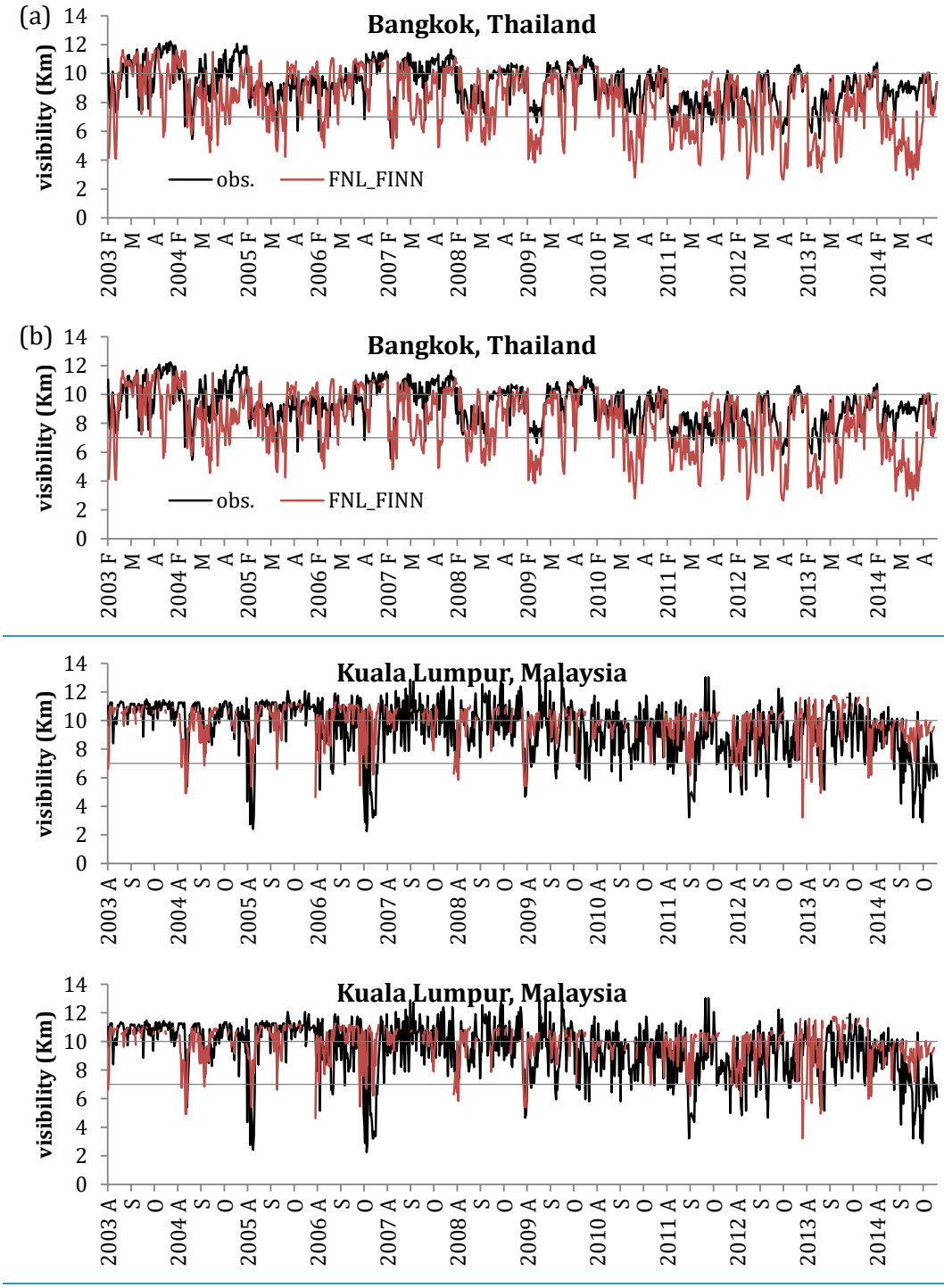
(a)
Bangkok, Thailand
visibility (Km)
obs.
FNL_FINN
(b)
Bangkok, Thailand
visibility (Km)
obs.
FNL_FINN
Kuala Lumpur, Malaysia
visibility (Km)
Kuala Lumpur, Malaysia
visibility (Km)

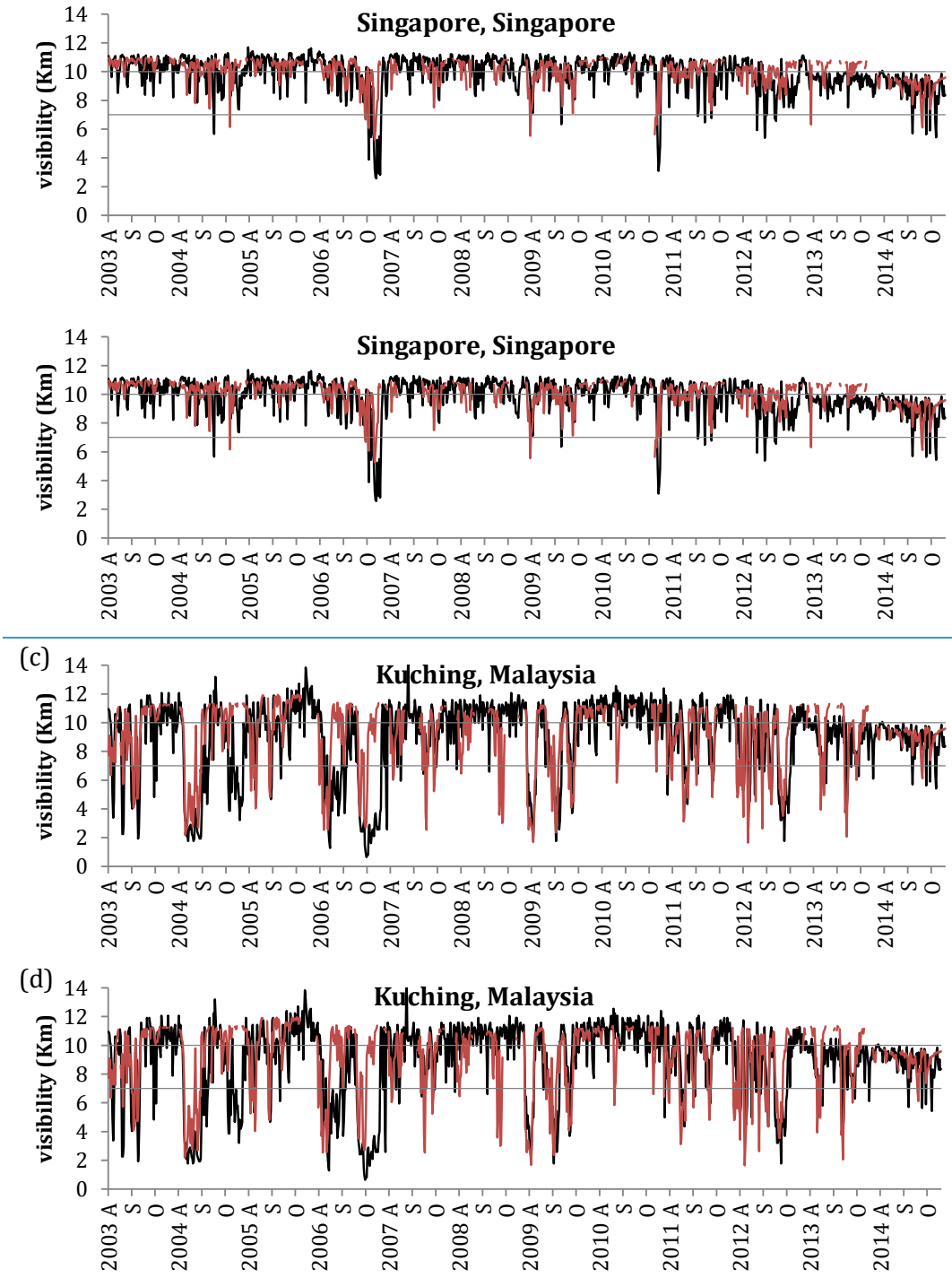

Figure 5. Comparison of daily visibility between GSOD observation (black lines) and FNL_FINN modeled result (red lines) in: (a) Bangkok, (b) Kuala Lumpur, (c) Singapore, (d) Kuching during the fire seasons from 2003 to 2014. Two grey lines mark the visibility of 7 and 10 km, respectively. F, M and A in the x-axis of (a) indicates February, March

and April, respectively. A, S and O in the x-axis of (b) – (d) are August, September, and October, respectively.

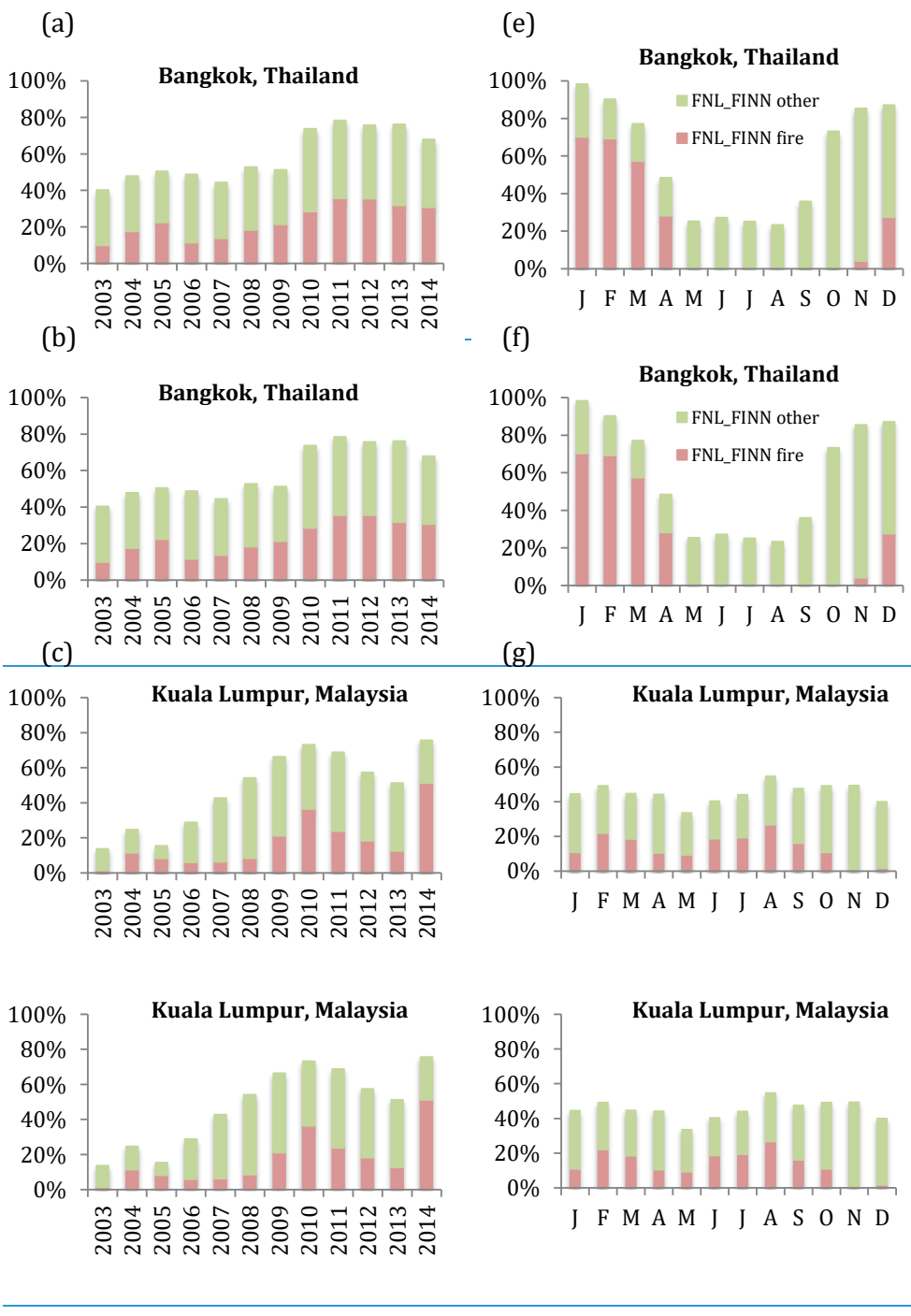
(a)
Bangkok, Thailand
100%
80%
60%
40%
20%
0%
2003
2004
2005
2006
2007
2008
2009
2010
2011
2012
2013
2014
(e)
Bangkok, Thailand
FNL_FINN other
FNL_FINN fire
J F M A M J J A S O N D
(b)
Bangkok, Thailand
(f)
Bangkok, Thailand
(c)
Kuala Lumpur, Malaysia
(g)
Kuala Lumpur, Malaysia
Kuala Lumpur, Malaysia
Kuala Lumpur, Malaysia

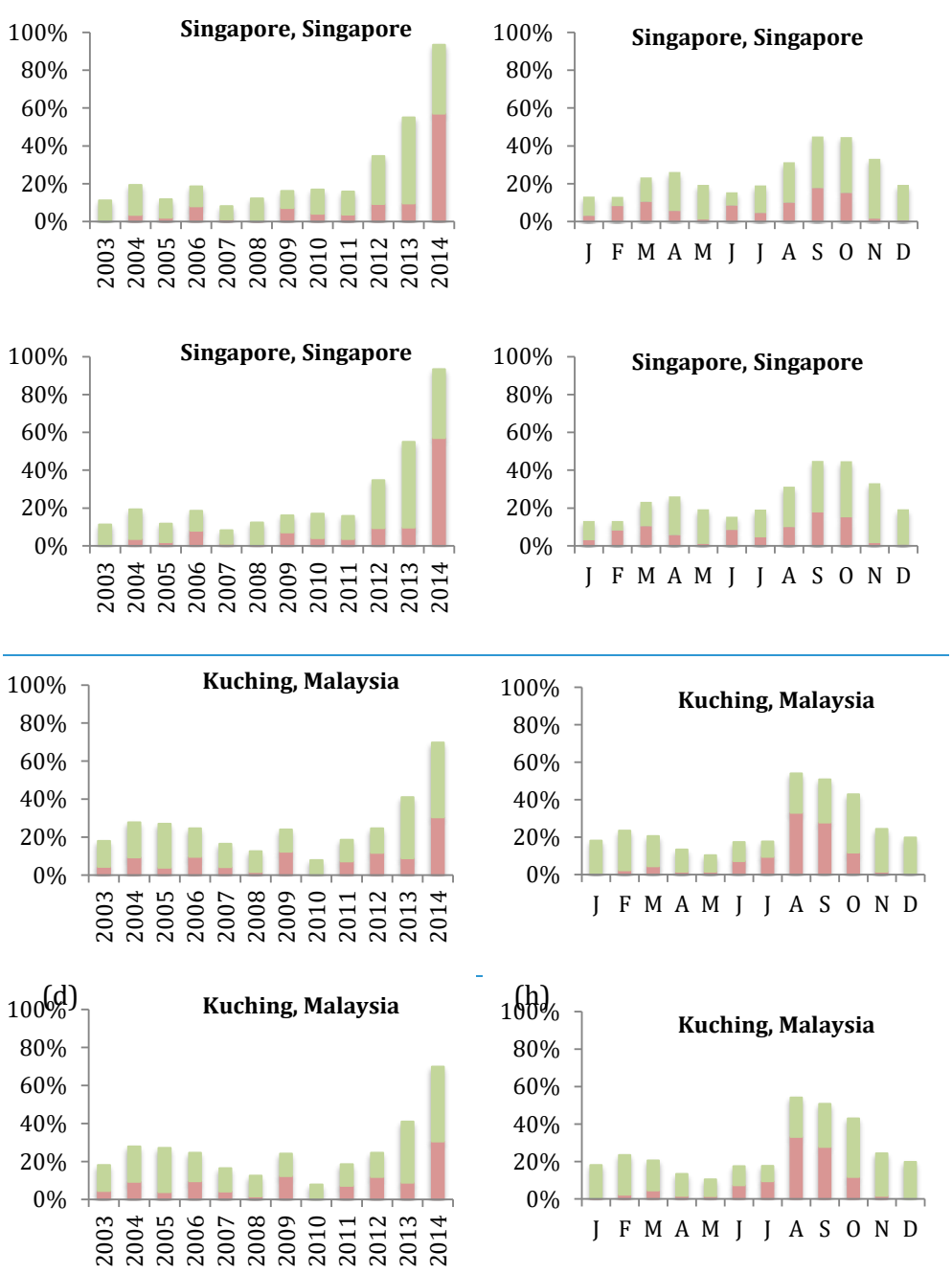

Figure 6. (a) – (d) The percentage of LVDs per year derived using from GSOD visibility observations in Bangkok, Kuala Lumpur, Singapore, and Kuching, respectively. (e) – (h) The percentage of LVDs averaged over 2003-2014, derived using GSOD visibility observations in Bangkok, Kuala Lumpur, Singapore, and Kuching, respectively. Each bar presents the observed LVDs in each year or month. Red color shows the partition of fire-caused LVDs (captured by model) while green color presents ~~non-fire~~other LVDs (observed – modeled; i.e. those not captured by model).

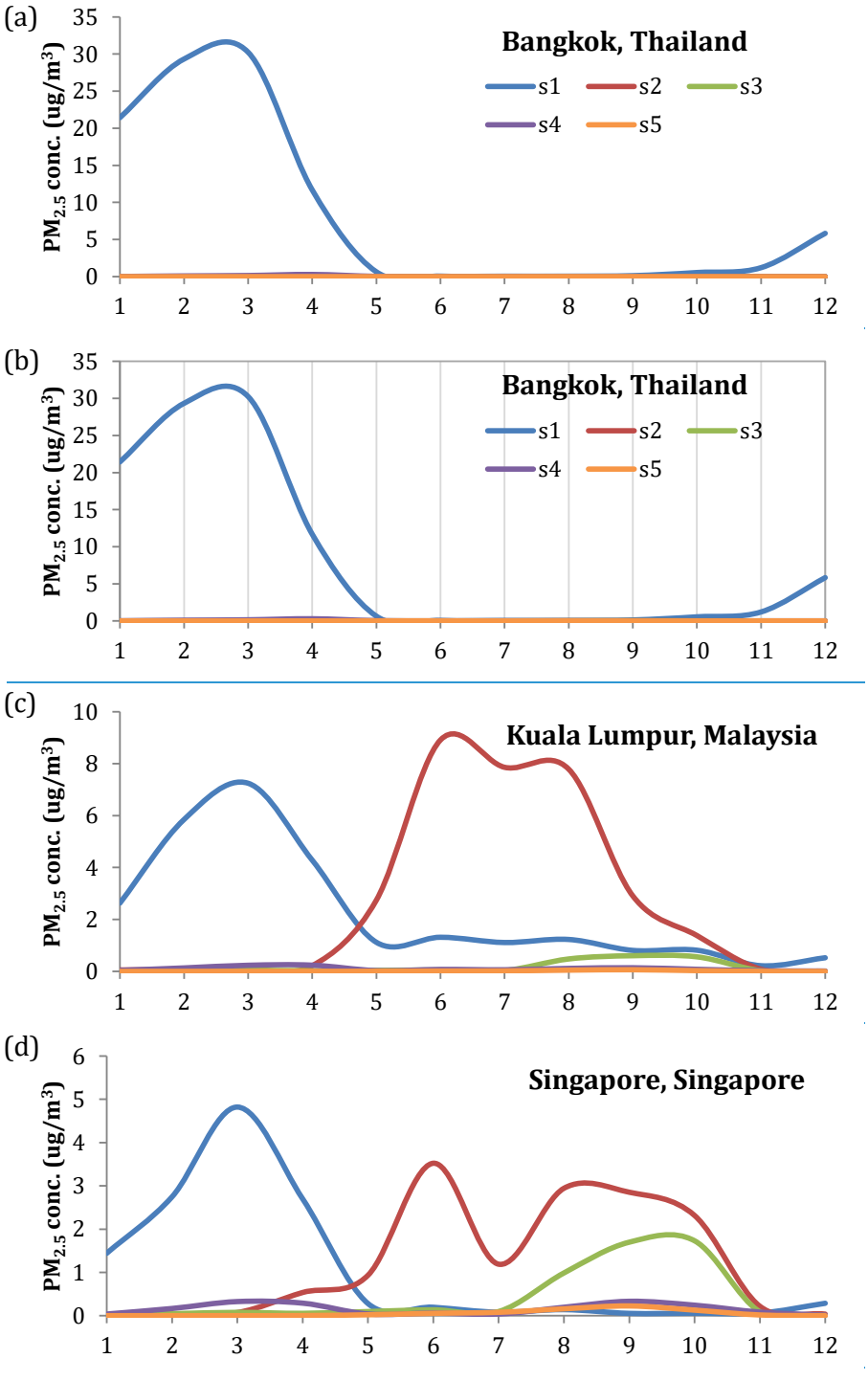
(a)
Bangkok, Thailand
s1
s2
s3
s4
s5
PM2.5 conc. (ug/m3)
(b)
Bangkok, Thailand
(c)
Kuala Lumpur, Malaysia
(d)
Singapore, Singapore

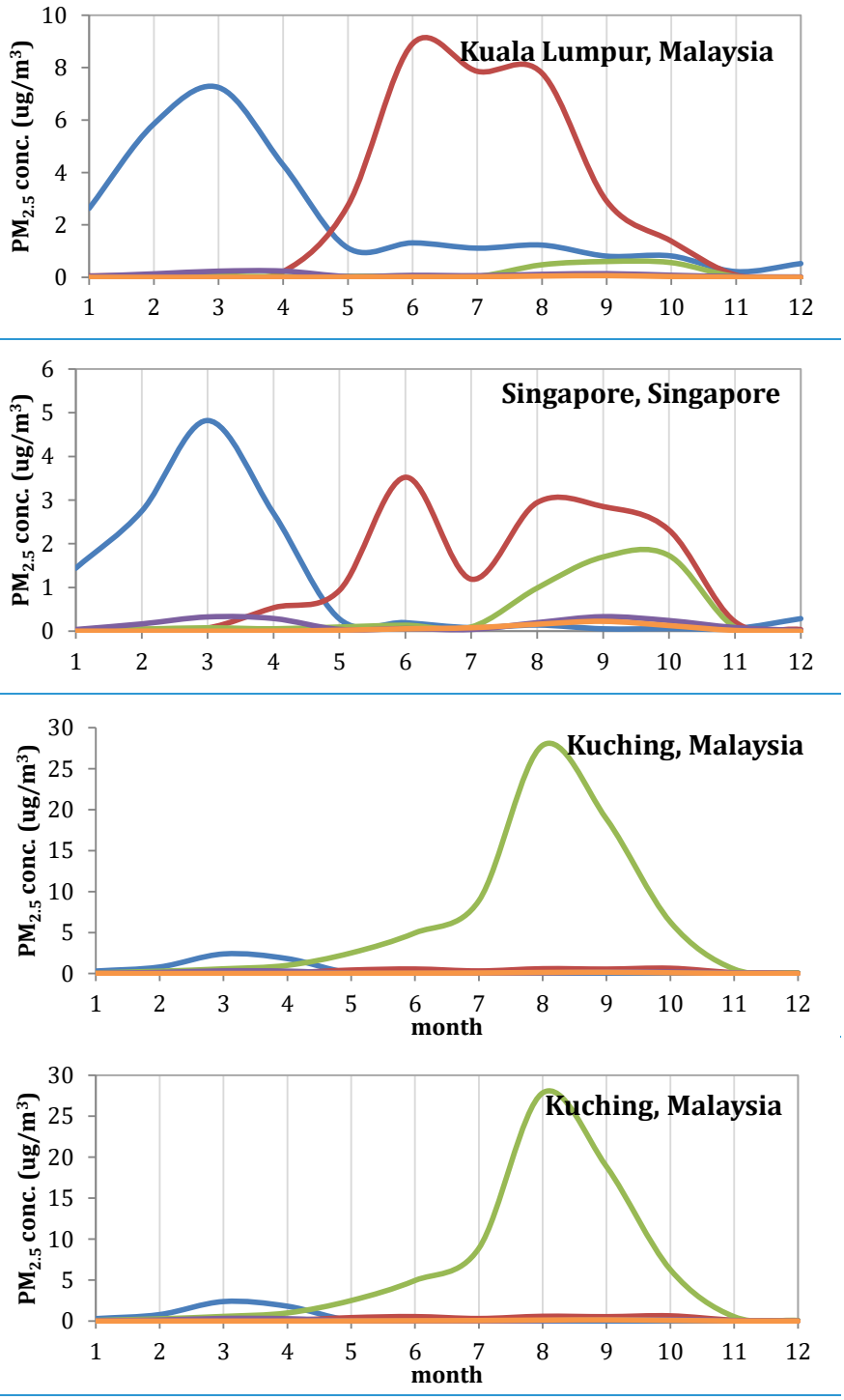

Figure 7. The mean fire $PM_{2.5}$ concentrations within the PBL attributed to different emission regions (s1 - s5) in (a) Bangkok, (b) Kuala Lumpur, (c) Singapore and (d)

Kuching, all derived from FNL_FINN simulation and averaged over the period of 2003-2014.

1175

(a)

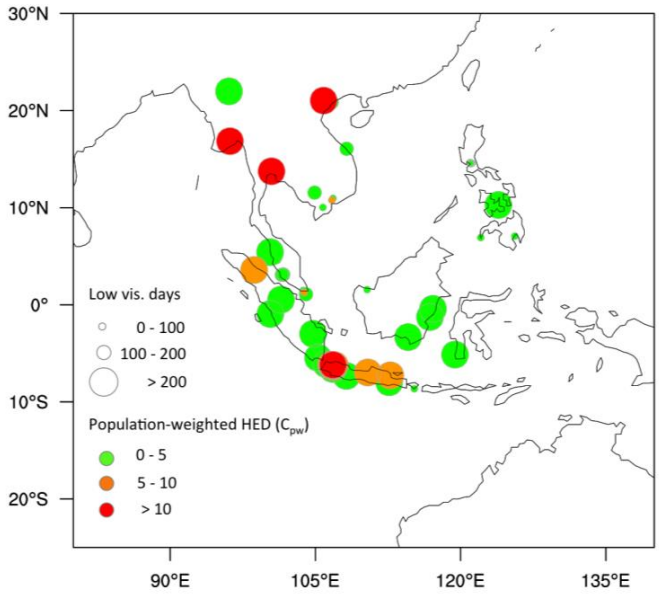

(b)

1176

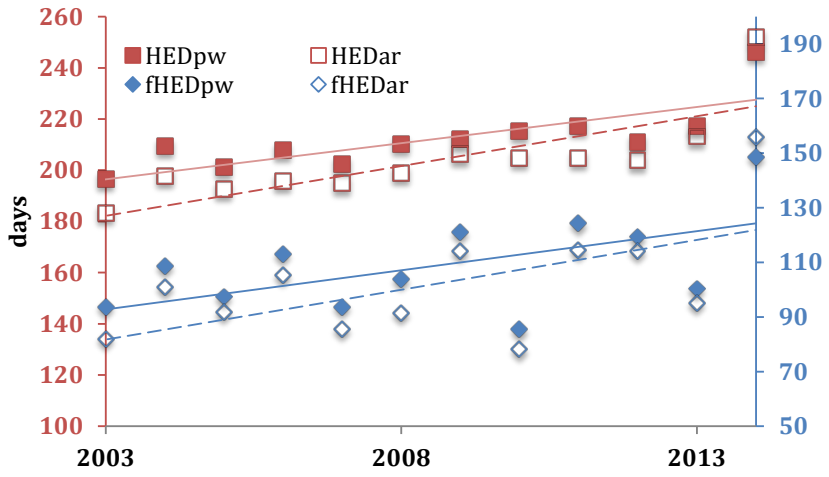

1177

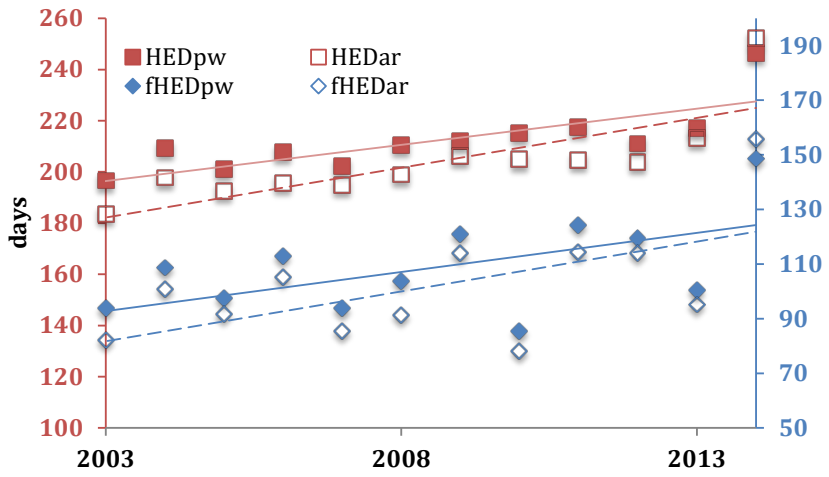

Figure 8. (a) The mean low visibility days (circles) per year from 2003 to 2014 in 50 ASEAN cities. The size of the circles indicates the number of days. The colors refer to population-weighted fraction in the total Haze Exposure Days (HED). (b) Annual population-weighted HED (HED_{pw}) and arithmetic mean HED (HED_{ar}). Fire-caused HED are labeled as $fHED_{pw}$ and $fHED_{ar}$. Units are in days. Note that the y-axes are in different scales.

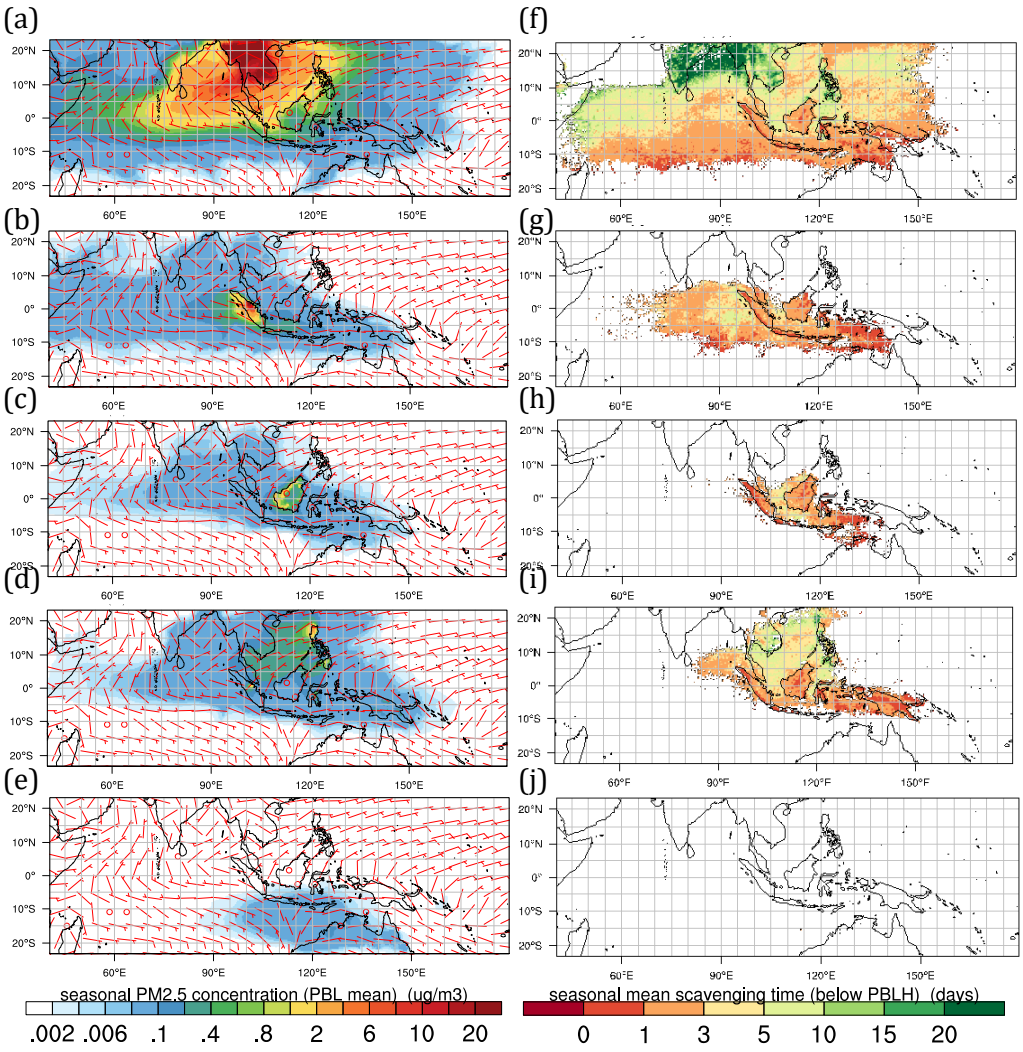

Figure 9. Seasonal mean fire $PM_{2.5}$ concentration (μg m^{-3}) and wind within the PBL modeled in FNL_FINN during February to April, 2003–2014 for fire $PM_{2.5}$ source region from (a) mainland Southeast Asia, (b) Sumatra and Java islands, (c) Borneo, (d) the rest of the Maritime Continent, and (e) northern Australia. (f)-(gj) Same as (a)-(e) but for seasonal mean wet scavenging time (days).